

Assessment of extreme hydrological conditions in the Bothnian Bay, Baltic Sea and the impact of the nuclear power plant "Hanhikivi-1" on the local thermal regime

Anton Yu. Dvornikov¹, Stanislav D. Martyanov¹, Vladimir A. Ryabchenko¹, Tatjana R. Eremina²,
5 Alexey V. Isaev¹, Dmitry V. Sein³

¹ The St.-Petersburg Branch of the P.P. Shirshov Institute of Oceanology, Russian Academy of Sciences, 1 Liniya V.O., 30, 199053, St.-Petersburg, Russia

² Russian State Hydrometeorological University, Malookhtinsky prospect, 98, 195196, St.-Petersburg, Russia

³ Alfred Wegener Institute, Helmholtz Centre for Polar and Marine Research, Postfach 120161, Am Handelshafen 12, 27570
10 Bremerhaven, Germany

Correspondence to: Dmitry Sein (dmitry.sein@googlemail.com)

Abstract. The results of the study aimed to assess the influence of future nuclear power plant "Hanhikivi-1" upon the local thermal conditions in the Bothnian Bay in the Baltic Sea are presented. A number of experiments with different numerical models were also carried out in order to estimate the extreme hydro-meteorological conditions in the area of the
15 construction. The numerical experiments were fulfilled both with analytically-specified external forcing and with real external forcing for two years: a cold year (2010) and a warm year (2014). The study has shown that the extreme values of sea level, water temperature, the characteristics of wind waves and sea ice in the vicinity of the future nuclear power plant can be significant and sometimes catastrophic. Permanent release of heat into the marine environment from operating nuclear power plant will lead to a strong increase in temperature and the disappearance of ice cover around 2 km vicinity of
20 the station. These effects should be taken into account when assessing local climate changes in the future.

1 Introduction

In recent decades the use of nuclear energy has been extending to a large scale. New nuclear power plants (NPPs) are designed and constructed, including those situated on the shores of the seas and oceans, which provides free access to water needed for cooling processes as discussed in (Rubbelke and Vogele, 2010). However, during the construction of this
25 kind of objects it is absolutely necessary to carry out a preliminary examination, including the assessment of risks associated with extreme natural conditions that may lead to technogenic disasters, as recently happened at the Japanese NPP in Fukushima, damaged during the earthquake and the subsequent tsunami (see Acton and Hibbs, 2012; Buesseler et al., 2011; Srinivasan and Gopi Rethinaraj, 2013). There exists a twofold oppositely directed influence: 1) NPPs are affected by the environment, 2) NPPs have impact on the environment with possible negative effects manifested, in particular, in the release
30 of warm cooling water (Chuang et al., 2009; Thermal standards for cooling water..., 2011).

Ensuring the safety of the operation of existing and planned NPPs requires solving the following two scientific problems: 1) evaluation of extreme external conditions (meteorological, hydrological, seismic) followed by an assessment of their impact on the NPPs, and 2) producing Environmental Impact Assessment (EIA) for NPPs. In contrast to the first problem, which has been studied extensively in meteorology and oceanography in recent decades, researches on EIA
35 methods, especially for the marine environment in the case of existing and planned NPPs operating in a regular mode, are not too numerous (see, for example, Zeng et al., 2002; Abbaspour et al., 2005; Kaplan et al., 2016).

The environmental impact of a NPP results from the nuclear fuel cycle, the effects of nuclear accidents, and NPP operation. It is known that the greenhouse gas emissions from nuclear fission power are much smaller than those associated with coal, oil and gas, and the routine health risks are much smaller than those associated with coal. However, there is a
40 "catastrophic risk" potential if containment fails (von Hippel, 2010), which in nuclear reactors can be brought about by over-

heated fuels melting and releasing large quantities of fission products into the environment. This potential risk could wipe out the benefits. Some predictions of the impact of severe accidents at NPP on radionuclide contamination of the near-surface environment are given in (Rumynin, 2015).

5 The environmental impact of NPP due to operation has been studied less than nuclear fission effects. During the process of nuclear power generation large volumes of water are used. The uranium fuel inside reactors undergoes induced nuclear fission which releases great amounts of energy that is used to heat water. The water turns into steam and rotates a turbine, creating electricity. Nuclear plants must collect around 600 gallons/MWh for this process (Tellinghuisen, 2016), so the plants are built near bodies of water.

10 As with all thermoelectric plants, NPPs need the cooling systems. The most common systems for thermal power plants, including nuclear, are:

- Once-through cooling, in which water is drawn from a large water body, passes through the cooling system, and then flows back into the water body.

- Cooling pond, in which water is drawn from a pond dedicated to the purpose, passes through the cooling system, and then returns to the pond.

15 • Cooling towers, in which water recirculates through the cooling system until it evaporates from the tower.

Nuclear plants exchange 60 to 70 % of their thermal energy by cycling with a body of water or by the evaporation of water through a cooling tower. According to the World Nuclear Association data (<http://www.world-nuclear.org>), this thermal efficiency is somewhat lower than that of coal-fired power plants, thus creating more waste heat.

20 When intaking water for the cooling process, nuclear plants, like all thermal power plants, use special structures. Water is often drawn through screens to minimize the entry of debris. The problem is that many aquatic organisms are trapped and killed against the screens, through a process known as impingement. Aquatic organisms small enough to pass through the screens are subject to toxic stress in a process known as entrainment. Billions of marine organisms, such as fish, seals, shellfish, and turtles, essential to the food chain, are sucked into the cooling systems and destroyed.

25 The long-term experience related to the world-wide operating of NPPs shows that, under normal safe operating conditions, the non-radiological impact on the environment becomes dominating. One of the major factors is the heat pollution of the surface water bodies due to the discharge of waste heat from the condensers of NPPs. If heated condenser water is not cooled for re-use in a cooling tower, the waste heat may be discharged either into artificial reservoirs (ponds) or directly into surface waters like rivers, lakes, and sea bays.

30 Nuclear power plants, among other things, release the warm water into the sea, which can significantly affect the functioning of marine ecosystems on a local scale. In (Hong and Guixiang, 2012) a significant negative impact of the warm cooling waters ejection of the coastal power plant located in the tidal Xiangshan Bay (China) on phytoplankton was shown. Similar conclusions are given in (Chuang et al., 2009) after the assessment of the impact of discharged water from a coastal nuclear power plant located in Taiwan. Also the impact assessment of the discharged water from a nuclear power plant located on the Atlantic coast in Brazil (Ilha Grande Bay) has shown the changes in the composition and structure of marine fish species as it was shown by (Teixeira et al., 2009). All the studies were carried out on the basis of field measurements and observations.

40 In the work by (Bork and Maier-Reimer, 1978) by means of numerical simulation the thermal regime in the tidal river Elbe was reproduced. As it was expected, the results showed a clear oscillatory nature of the spread of the warm water induced by the tidal currents. It can be assumed that, in contrast to the spread of the heated water in the tidal river which always has its own flow velocity, in tidal coastal area the oscillating contribution would be more pronounced. In (Abbaspour et al., 2005) the modeling of the warm waters spread from the coastal thermal power plant (Bandar Abbas Thermal Power Plant, BATP) located in the Persian Gulf was carried out and shown good results of this method in the prediction of the discharged water spread in the basin with strong tidal oscillations. In the work by (Zeng et al., 2002) the physical and

numerical modeling of the warm discharged water transport spreading from a coastal nuclear power plant located in the tidal area of Daya Bay (China) near Hong Kong was carried out and also performed good results in the simulation of the studied process.

5 Beside the field observations and numerical modeling, the usage of the satellite data can also be useful in such assessments, as it was shown, for example, in the work by (Chen et al., 2003) presenting the analysis of thermal pollution from a nuclear power plant located on the shores of the tidal South China Sea. The paper noted that it is more difficult to evaluate the effect of thermal pollution from a power plant that in tidal seas than in non-tidal.

10 At present, there are five operating NPPs on the shores of the Baltic Sea: two Swedish (Forsmarks NPP, the electric capacity of 3210 MW, Oskarshamn, 2308 MW), two Finnish (Loviisa NPP, 1020 MW, Olkiluoto NPP, 1760 MW) and one Russian (Leningrad NPP, 4000 MW). Two of them (Forsmark and Olkiluoto) are located on the coast of the Bothnian Sea. On January 19, 2016, the construction of NPP "Hanhikivi-1" with the capacity of 1200 MW was started. This event had been preceded by examination of hydro-meteorological conditions in the area of construction, which included not only the estimation of extreme conditions in the vicinity of Peninsula Hanhikivi (Pyhäjoki municipality) in the Bothnian Bay in the Baltic Sea, but also the possible impact of future power plant on the marine environment in this area.

15 In particular, the evaluation of extreme weather and sea events in the Bothnian Bay in the case of the absence of the NPP was carried out by the Swedish Meteorological and Hydrological Institute (SMHI, 2014). To find the extreme values of sea temperature and water level SMHI used long time series of observations of these characteristics complemented by the results obtained by HIROMB runs with horizontal resolution of 1×1 nautical mile and vertical resolution of 4-8 m. The analysis was limited by the period of 1990-2011 in the case of temperature and by the whole period of observations in the case of water level. The similar assessment was made by the company Fennovoima Oy with making use of only available observational data in the area of the planned construction (Fennovoima report, 2015; Alenius, 2015). Both estimates are based on statistical methods by means of which the maximum and minimum values and the extremes probability and frequency were calculated. As for the EIA of the proposed NPP, those estimates were usually based on the observational data, as well as on simple dispersion models for jet propagation in liquid and expert assessments (Fennovoima report, 2014) and thus both estimates can be considered as preliminary and indicative. The method proposed below which is based on three-dimensional modeling of hydrodynamics on ultra-high resolution grids provides more reliable assessments.

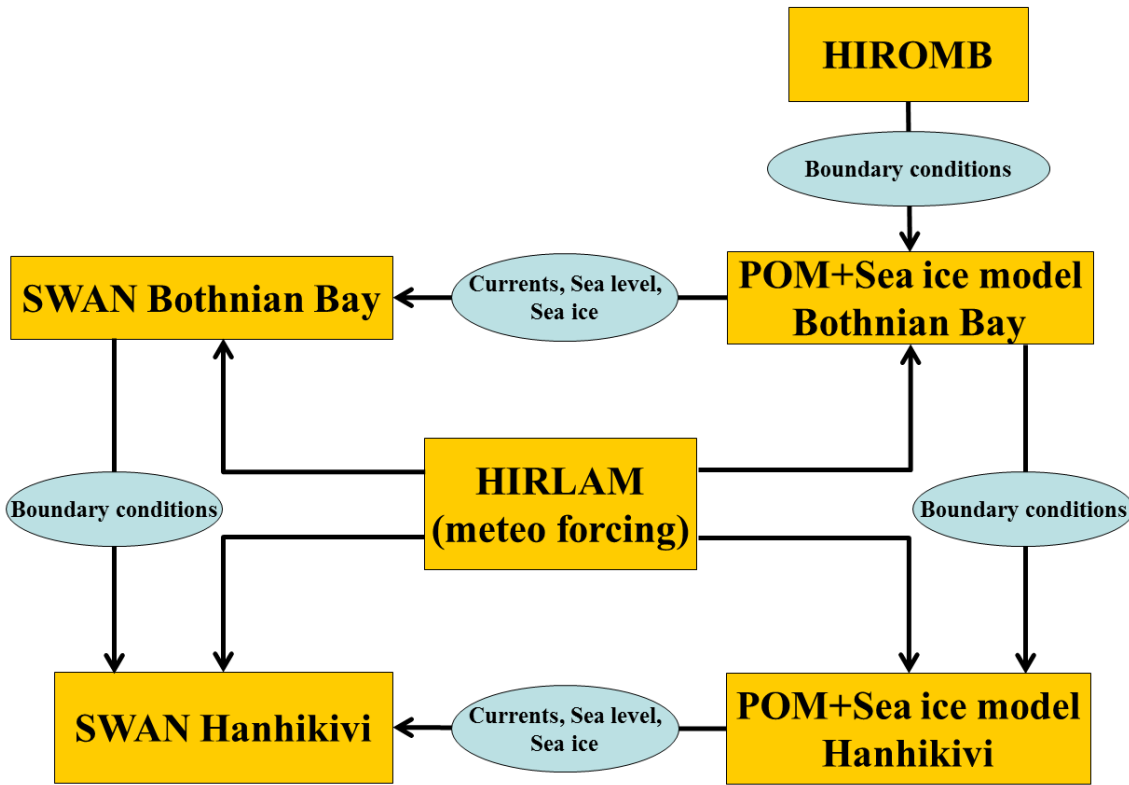
The purpose of this study was two-fold: 1) to estimate the possible extreme marine phenomena in this region (wind waves, sea level changes); 2) to estimate the impact of the NPP on the local thermal regime in the future. To do this, we used different hydrodynamic models. Results of this examination are presented below.

30 **2 Methods**

When evaluating extreme hydro-meteorological conditions in the study area of the sea an empirical approach based on statistical analysis of the available time series of individual characteristics (wind speed, sea level, water temperature, ice cover characteristics, and others) is traditionally used. This approach has at least two obvious limitations: 1) the accuracy of such estimates is highly dependent on the duration of the observation period; 2) it cannot be used for areas where such data is not available. In this paper we propose a method of extreme hydrological conditions estimation in the study area based on mathematical modeling of the general ocean circulation. In the present study, the extreme hydrological conditions in the area of the future NPP "Hanhikivi-1" are estimated in the Bothnian Bay in the Baltic Sea. The general scheme of the calculation is as follows: 1) to perform a model run to simulate the general circulation for the entire Bothnian Bay on the coarse grid for the selected period (from 2010 to 2015 with repetition 2 times of the 2010 year under one and the same external forcing) including the cold (2010) and the warm (2014) years in the situation of the absence of the NPP; the model performance is verified through the quality of simulation of temperature and sea ice area fields; 2) to assess the extreme possible sea level in the NPP area on the basis of runs on the coarse grid. For this purpose the real situations of extreme storm surges during the

selected time period were chosen 3) to assess the impact of the NPP on the temperature and sea ice fields around it on the basis of performing the calculations in the case of the absence of the NPP ("background" scenario) and its presence ("predictive" scenario); runs are performed on the nested (fine) grid covering the neighborhood of the NPP for both cold and warm years; 4) to assess the largest wind waves by performing the numerical experiments first on the coarse grid, and then on the fine grid with the prescribing boundary conditions from the solutions on the coarse grid.

The general scheme of numerical experiments is shown in Fig. 1. The models used and the details of the above numerical experiments are specified below.



10 **Figure 1: The general scheme of the model calculations.**

2.1 Circulation model

A three-dimensional numerical model based on the Princeton Ocean Model (POM) (Blumberg and Mellor, 1987; Mellor, 2004) was used to simulate the circulation pattern and thermal regime in the Bothnian Bay. It is a model with a σ -coordinate in the vertical direction that allows a smooth representation of the bathymetry and provides a better simulation of the currents in the bottom boundary layer as compared with some z- and isopycnal models. Also such σ -models reproduce different thermodynamic effects caused by the non-linearity of the equation of state rather well. That is why such models have been widely used for the simulations of coastal and estuarine dynamics. As for the turbulence closure parameterization, POM makes use of the well-tested and reliable schemes of Mellor-Yamada 2.5 (Mellor and Yamada, 1982) for the vertical, and Smagorinsky (Smagorinsky et al., 1965) for the horizontal turbulent mixing, respectively. The above-mentioned advantages of the model along with the significant experience of the authors with its use in a number of successful applications for other basins in similar studies (Ryabchenko et al., 2008) were the main reasons why POM was chosen for the present study. The model allows to simulate three-dimensional fields of currents, water temperature and salinity, two-dimensional elevation field in an area of interest when external influence is specified. This influence includes wind forcing, sea-surface atmospheric pressure, air temperature and humidity in the near-water layer, cloudiness, precipitation rate and open boundary conditions.

2.2 Sea-ice and snow model

To model ice and snow distribution in any area an advanced sea-ice model with several different categories of ice was used (Haapala et al., 2005; Ryabchenko et al., 2010). The model distinguishes the sea ice as two main types: deformed and non-deformed. The non-deformed ice is divided into several sub-categories, while the deformed ice consists of only ridged and rafted ice. The rafted ice exists when the ice thickness is equal or less than 17 cm, otherwise the ice is considered to be ridged. Evolution of each type is described by ice concentration and mass equations. The ice thickness of each category varies due to advection, deformation and thermodynamic processes. It is assumed that the fast ice exists in the areas with the depth less than some specified value. But in the present study the fast ice was not considered, and the model operated with 7 different categories of sea ice.

The evolution of snow cover thickness can be described as the interaction of the following main mechanisms (Lepparanta, 1983): precipitation, surface melting, compaction, and the formation of slush, which further transforms into snow-ice. In the present model only the precipitation and surface melting were taken into account (Ryabchenko et al., 2010).

2.3 Wind waves model

The wind waves model SWAN (Simulating WAVes Nearshore) (Booij et al., 1999; Ris et al., 1999) was used in the present study. SWAN is a third-generation spectral wave model specifically developed for wind waves simulation in shelf and shallow coastal areas with complex shore line configuration. The model can take into account wind forcing, depth-induced wave breaking, refraction, diffraction, ambient currents and sea-level oscillations, bottom friction, white-capping, wave quadruplets and triads, wave-induced set-up, presence of sub-grid obstacles, vegetation and bottom mud layer, and also the turbulent viscosity. The core element of SWAN is the numerical and efficient solving of the spectral wave action balance equation, which includes source terms representing the effects of generation, dissipation and nonlinear wave-wave interactions.

SWAN was used in a non-stationary mode with a time step equal to 10 minutes, with maximal iterations at each time step set equal to 10. According to the recommendations presented in the official SWAN manual, the directional resolution was set equal to 10 degrees, minimal and maximal frequencies were set equal to 0.04 and 1.0 Hz, respectively.

2.4 Areas of interest and model domains

The present study focuses on the Bothnian Bay (a northern part of the Baltic Sea) and the relatively small area off the Hanhikivi peninsula located at the eastern coast of the Bothnian Bay (Fig. 2). The bathymetry data were collected from different marine navigational charts, from Baltic Sea Bathymetry Database (Baltic Sea Hydrographic Commission, 2013), and were provided from field observations. These data were linearly interpolated into grid nodes with further making use of low-frequency filter.

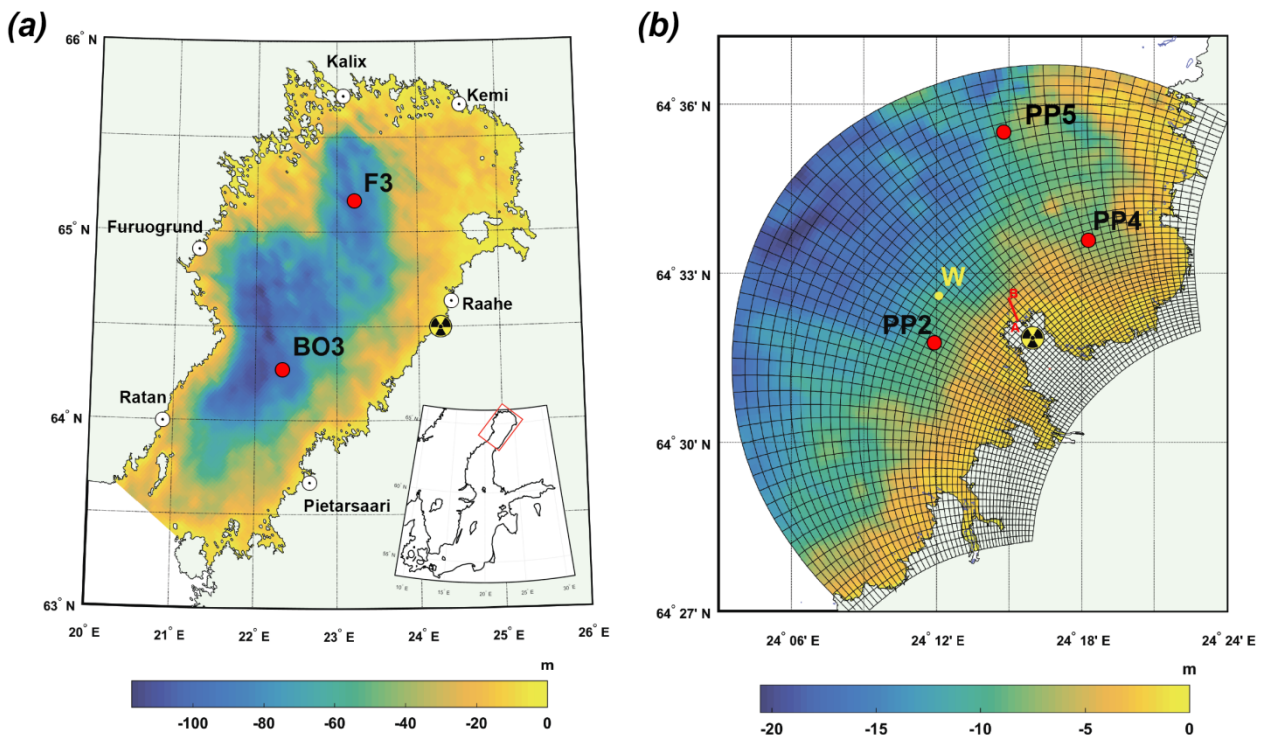


Figure 2: Bathymetry of the Bothnian Bay (a) and the area off the Hanhikivi peninsula (b). The location of the NPP, oceanographic stations (BO3, F3, PP2, PP4, PP5), coastal sites of sea-level measurements (Ratan, Furuogrund, Kalix, Kemi, Raahе, Pietarsaari) and also the position of cross-section (red line) and SWAN output point (W) are presented. The inset in the fragment (a) shows the position of the Bothnian Bay in the Baltic Sea.

The Bothnian Bay model grid consists of 107×175 nodes in horizontal and 25 sigma-levels in vertical direction, horizontal resolution being one nautical mile and minimum depth being 3 m. The model time step was set equal to 300 seconds.

The Hanhikivi area model grid is much more curvilinear in its shape (see Fig. 2b), consists of 142×193 nodes in horizontal and 12 sigma-levels in vertical direction. Its horizontal resolution is rather variable, the minimum and maximum horizontal resolution being 35 and 180 m, respectively. The minimum depth was set equal to 1.5 m and model time step was 0.5 second. The Hanhikivi model grid covers the area with radius app. 9000 m from the future NPP "Hanhikivi-1".

In addition to these above-mentioned main model domains and their grids we also built and used another grid which covered both the Bothnian Sea and the Bothnian Bay in order to assess the impact of incoming wind waves traveling from the Bothnian Sea northward into the Bothnian Bay through the open south boundary. This model grid (not shown) consisted of 101×250 nodes, the minimum depth was limited by the 3 m isobath, horizontal resolution: minimum 2.2 km, maximum 5.3 km. The main outcome obtained from the numerical experiments performed on this grid was that the impact of the incoming wind waves plays an important role only in the southern part of the Bothnian Bay and that its contribution to the wind waves pattern in the vicinity of Hanhikivi peninsula is negligible. Such result allowed us to concentrate only on the modeling efforts inside the Bothnian Bay without any need to include the Bothnian Sea into the model domain in all subsequent model runs, thus enhancing the model resolution and reducing the model total integration time.

2.5 Atmospheric forcing, boundary and initial conditions

Atmospheric forcing included air temperature and humidity, wind speed and direction, cloudiness, which were obtained from the results of atmospheric model HIRLAM (High Resolution Limited Area Model) (<http://hirlam.org>) provided to Russian State Hydrometeorological University by the Danish Meteorological Institute. HIRLAM's horizontal resolution is 11 km and the model's domain covers the North Atlantic and Northern Europe regions. To compare HIRLAM

results with measurements observational data on the meteorological station Raahe were used. These data represent the 3-hour monitoring data on air temperature and atmospheric pressure for the period from 01.01.2010 to 31.12.2014, and on the characteristics of wind speed for the period from 22.10.2010 to 31.12.2014. For the same period similar HIRLAM characteristics were made. The model and the observed values were averaged with a daily period. Table 1 shows the statistical characteristics of the observed and model values from year to year, Fig. 3 shows a comparison of calculated and observed mean monthly values of meteorological characteristics in 2010-2014. As it can be seen, there is a good agreement between the model and the observed values and thus the HIRLAM atmospheric forcing can be used in the simulation of hydrodynamic regime of the Bothnian Bay near the future NPP location.

10 **Table 1: Statistical characteristics of air temperature, atmospheric pressure and wind speed in the surface layer of the atmosphere between 2010 and 2014, calculated on the average daily data**

Years	Air temperature, °C		Atmospheric pressure, mb		Wind velocity, m c ⁻¹	
	Observations	HIRLAM	Observations	HIRLAM	Observations	HIRLAM
	Mean annual value					
2010	2.1	2.0	1012.2	1012.6	5.5	4.7
2011	4.6	3.7	1009.0	1009.5	6.3	5.5
2012	3.1	3.2	1010.3	1010.7	5.8	6.1
2013	4.7	4.7	1010.2	1010.6	6.2	6.1
2014	5.2	5.1	1012.8	1013.0	6.1	6.1
	Minimum value					
2010	-27.4	-26.5	981.8	981.6	1.5	1.1
2011	-25.6	-26.9	969.3	970.4	1.2	0.9
2012	-24.7	-26.1	973.2	973.4	1.7	1.9
2013	-19.2	-20.1	974.9	976.1	2.0	1.0
2014	-20.0	-21.9	976.5	977.3	1.7	1.6
	Maximum value					
2010	26.0	24.7	1046.8	1046.3	11.6	13.1
2011	25.6	20.4	1037.4	1038.0	18.9	17.2
2012	20.1	20.1	1056.0	1055.7	13.2	14.6
2013	21.4	21.3	1033.6	1033.9	17.7	18.1
2014	25.8	24.7	1040.6	1040.1	14.7	15.6
	Standard deviation					
2010	11.4	12.0	11.3	11.2	2.2	2.1
2011	9.9	9.0	12.8	12.7	2.8	2.9
2012	9.7	9.9	13.0	12.9	2.3	2.5
2013	9.4	9.2	10.7	10.7	2.5	2.8
2014	8.8	9.1	11.8	11.6	2.7	2.8

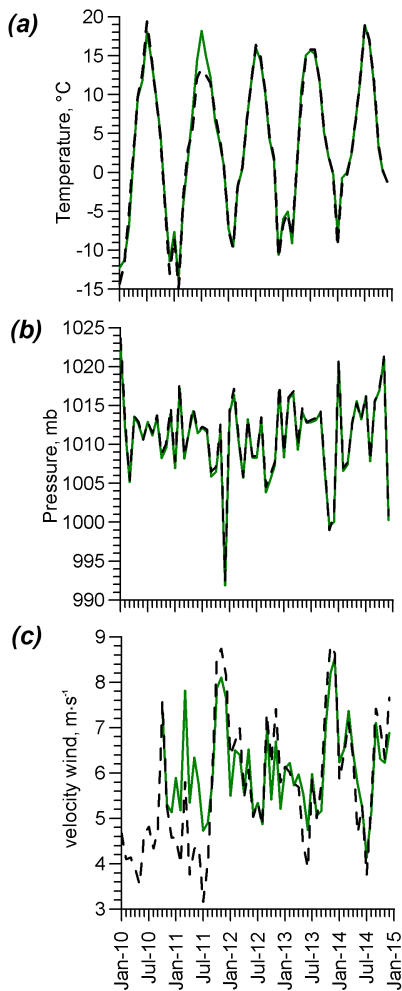


Figure 3: Temporal variability of mean monthly values of (a) air temperature ($^{\circ}\text{C}$), (b) atmospheric pressure (mb) and (c) wind speed (m s^{-1}) in the near-surface layer of the atmosphere. HIRLAM (dashed curves), observations (green curves).

5 The circulation model used in the present study calculates the momentum, heat and salt fluxes at the air-sea and air-ice interfaces. The momentum fluxes are calculated traditionally as a quadratic friction law making use of different drag coefficients for air-water, air-ice and ice-water boundaries. The heat and salt fluxes are parameterized by taking into account the diurnal cycle of short-wave solar radiation (Parkinson and Washington, 1979; Ryabchenko et al., 2010).

10 At the open boundaries the coupled circulation and sea-ice model assimilates the sea level, current velocity, water temperature and salinity, sea ice thickness and concentration, snow thickness obtained from the results of HIROMB (High Resolution Operational Model for the Baltic) (Funkquist, 2001; <http://www.smhi.se/en/research/research-departments/oceanography/hiromb-1.8372>), a high-quality prognostic 3D ocean circulation model recommended for all states in the Baltic Sea region by Helsinki commission (HELCOM). HIROMB covers the North Sea and the Baltic Sea with horizontal resolution in the latter being one nautical mile and vertical resolution being 4 m (24 vertical levels). HIROMB
15 data also include river runoff in the Baltic Sea region.

 At the solid lateral boundaries (coasts) a no-slip condition and zero fluxes are specified for horizontal velocity, heat and salt, respectively.

 At the bottom the vertical component of current velocity, heat and salt fluxes are set to zero. Bed shear stress is parameterized as a function of horizontal velocity at the near-bed model sigma level.

20 All the above-described hydrological boundary conditions were applied for the Bothnian Bay circulation model, while for the Hanhikivi area circulation model the results obtained from the previous Bothnian Bay model runs were used as the boundary conditions, implementing nesting technique.

It should also be noted that the hydrological regime of the area located relatively close to the Hanhikivi peninsula is considerably affected by the river Pohjoishaara situated nearby and with an annual runoff equal to $103 \times 10^7 \text{ m}^3$. In the present study, for the Hanhikivi model the river Pohjoishaara runoff was distributed into 12 months in accordance with the known monthly averages of the nearest large rivers' runoff. The Pohjoishaara's water temperature was set to the nearest coastal area water temperature, while salinity was set to zero.

The initial conditions for the coupled circulation and sea-ice model for the entire Bothnian Bay domain included water temperature, salinity and sea level fields obtained from the HIROMB model.

Generally speaking, extreme sea levels in the Bothnian Bay are caused by storm winds, long waves, tides, low atmospheric pressure, seiches, and sea level rise of the World Ocean. Tidal level oscillations in the Gulf of Bothnia are negligible (Lepparanta and Myrberg, 2009) and can be omitted in model simulations. The influence of moving centers of the low atmospheric pressure has not been investigated in the present study, still it can be assumed that their impact is commonly appears jointly with the wind impact (SMHI, 2014). In order to simulate extreme sea level oscillations in the vicinity of the NPP "Hanhikivi-1" we considered the situations with constant (both in speed and direction) maximal possible wind blowing long enough to establish an equilibrium state and under the influence of sea level change caused by the long wave coming from the Baltic Sea. As indicated above, such a simplistic approach to the evaluation of extreme sea level in the area of interest gives results in good agreement with the estimates of extreme values of sea level according to the observations during almost 100 years.

For the SWAN model the initial condition of no waves in the entire domain was adopted. At the solid boundaries the model sets the condition of full wave energy absorption and no wave energy generation. At the open boundaries in the case of outgoing waves they can leave the area freely (radiation condition), while in the case of incoming waves there can be two options: 1) either no waves come into the model domain (an option used for the Bothnian Bay model) or 2) incoming wave spectrum is specified along the open boundary which has been obtained from the previous Bothnian Bay simulations (an option used for the Hanhikivi model).

The model estimates of wind waves characteristics took into account the possible presence of the sea-ice cover in the Bothnian Bay, which in reality hinders or prevents the free generation and propagation of surface waves and limits the wave fetch if some part of the basin is covered with ice. The model run for 2014 was fulfilled for the entire year that is why the inclusion of sea-ice into the wind waves model was necessary. We assumed the isoline of ice concentration equal to 0.5 as an edge of the ice cover that in fact was some kind of simplification but still appeared as an effective way to limit the wave fetch in the presence of sea-ice in the Bothnian Bay. All required data for the SWAN model (sea level oscillations, currents, sea-ice) had been calculated in advance by the coupled circulation model before being used in the SWAN model.

2.6 Verification of the models

Taking into account the main objective of this study - to estimate extreme values of the sea level and height of wind waves in the vicinity of NPP "Hankikivi-1" and estimate the maximum thermal pollution produced by the NPP, the proposed models were verified with respect to the sea level, significant wave height, sea water temperature and sea-ice area against all available observational data for the selected period 2010-2015. This data includes data on sea level at six stations (Ratan, Furuogrund, Kalix, Kemi, Raahe, Pietarsaari) on the shores of the Bothnian Bay (ftp://myocean.smhi.se/Core/INSITU_BAL_NRT_OBSERVATIONS_013_032/history/mooring/), vertical temperature profiles for hydrographic stations BO3, F3 (data from BED <http://www.balticnest.org/bed>) and PP5 (Fennovoima report, 2014), and data on the significant wave height at the stations PP2 and PP4 (Fennovoima report, 2013), the average monthly data on the area of the ice cover (<http://www.aari.ru/>).

2.6.1 Circulation model verification

Sea level. Model verification with respect to the sea level was carried out using the series of hourly sea level values for the period from 00 hours of 1 January 2010 to 23 hours of December 31, 2015, obtained from observational data and modeling results in the 6 stations mentioned above. Statistical characteristics (correlation coefficient R and standard deviation σ) of sea level at the coastal stations (Table 2) indicate that both models reproduce the level with high enough accuracy everywhere in the Bothnian Bay. The observed and calculated sea levels for the short periods of 14-16.10.2010 and 5-7.12.2015 at the station Raahe nearest to the NPP are presented as an example (Fig. 4). Although the two models underestimate the amplitude of sea level changes, they give in general the consistent results and reproduce the sea level changes with sufficient accuracy. These periods were chosen as periods of strong storm surges causing the large fall and rise of sea level, respectively, at station Raahe. The extreme high and low sea level values are estimated in section 3.1.2 using information about the initial conditions for the hypothetical calculations of extreme values of the level just for the moments of the beginning of these two periods.

Table 2: Statistical characteristics (correlation coefficient R and standard deviation σ) of water level at coastal stations in the Bothnian Bay in 2010-2015 according to observations, results from HIROMB and POM (this study)

Characteristic	R , data – POM	R , data – HIROMB	σ , m data	σ , m POM	σ , m HIROMB
Ratan	0.88	0.88	0.24	0.21	0.22
Furuogrund	0.88	0.89	0.25	0.22	0.24
Kalix	0.88	0.88	0.27	0.24	0.25
Kemi	0.89	0.90	0.28	0.25	0.27
Raahe	0.88	0.89	0.23	0.26	0.25
Pietarsaari	0.80	0.82	0.21	0.22	0.23

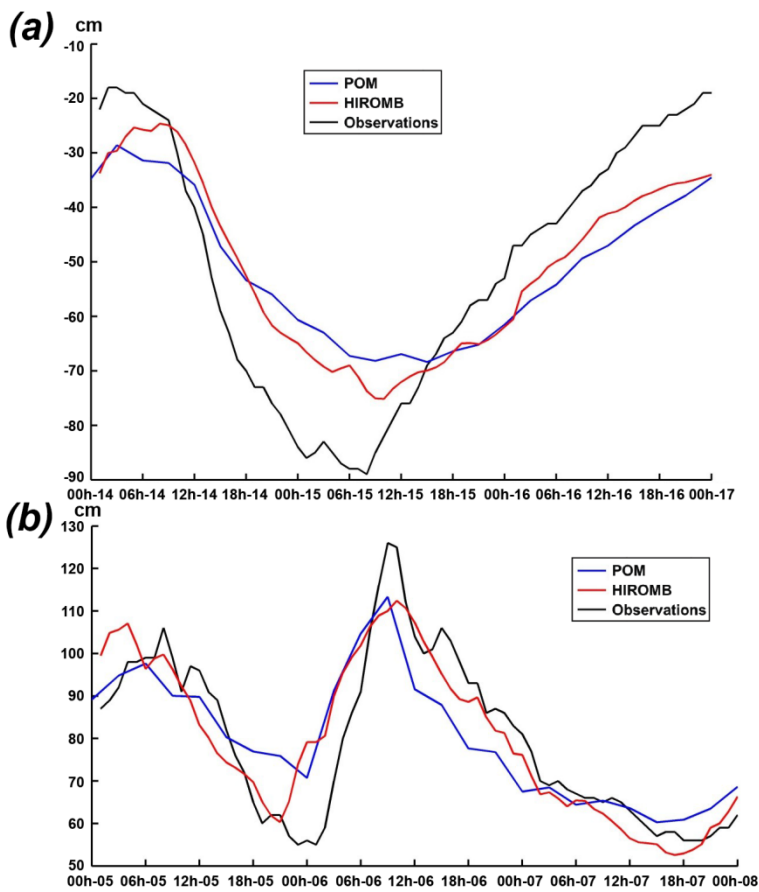


Figure 4: Comparison of POM and HIROMB calculated sea levels at station Raahe located near the NPP "Hankikivi-1" for the storm surge periods of 14-16.10.2010 (a) and 5-7.12.2015 (b).

5 *Temperature.* Comparison of the results of temperature simulation on the coarse grid with the available data of field observations in the Bothnian Bay from BED was performed for two stations: BO3 (64.30° N 22.35° E) and F3 (65.17° N 23.23° E). At these stations for the considered period in open access there are 40 vertical profiles of temperature: 12 for BO3 and 28 for F3. Comparison of mean values and standard deviations for the observed vertical profiles of temperature with the similar characteristics obtained on 2 nm grid using HIROMB, and on 1 nm grid using POM (this work) is presented in Table 3. Figure 5 shows the examples of profiles for both stations in January and June 2010.

Table 3. Statistical characteristics (mean value m and standard deviation σ) of vertical temperature profiles at the oceanographic stations BO3 and F3 in the Bothnian Bay in 2010-2012 according to BED observations, results from HIROMB and POM (this study)

Station Number	Station Name	Station Date	$m, ^\circ C$ Data	$m, ^\circ C$ HIROMB	$m, ^\circ C$ POM	$\sigma, ^\circ C$ Data	$\sigma, ^\circ C$ HIROMB	$\sigma, ^\circ C$ POM
1	BO3	2010-01-18	1.29	2.90	2.02	1.36	2.64	1.77
2	BO3	2010-01-18	0.60	1.44	0.53	0.56	1.43	0.57
3	BO3	2010-06-06	1.73	2.20	1.89	1.10	1.14	1.11
4	BO3	2010-08-22	4.05	6.50	7.11	4.80	5.16	4.56
5	BO3	2011-01-24	0.82	1.47	0.76	0.88	1.10	0.67
6	BO3	2011-05-29	1.30	1.92	1.76	1.01	1.56	1.23
7	BO3	2011-08-21	5.76	6.37	8.34	4.65	6.01	4.64
8	BO3	2012-05-31	1.99	2.71	2.93	1.07	1.49	1.17

9	BO3	2012-08-23	6.13	7.83	8.38	4.13	4.85	3.98
10	BO3	2010-12-02	3.61	2.91	3.01	0.44	1.14	1.32
11	BO3	2011-12-11	3.30	2.92	3.53	0.52	0.80	0.17
12	BO3	2012-12-10	3.58	3.93	4.08	0.39	1.21	1.21
13	F3	2010-01-19	1.74	2.45	2.41	1.53	2.22	2.47
14	F3	2011-01-24	0.95	1.14	1.27	0.93	1.08	1.29
15	F3	2010-03-05	0.41	2.14	1.81	1.12	2.28	1.79
16	F3	2010-03-23	0.73	1.91	1.92	1.09	2.04	1.95
17	F3	2010-05-05	0.92	2.44	2.29	1.11	1.94	1.67
18	F3	2010-05-19	1.29	2.22	2.20	0.88	1.78	1.44
19	F3	2010-06-09	3.74	3.53	2.94	2.79	0.34	0.72
20	F3	2010-06-30	5.30	5.76	5.07	4.24	2.71	2.75
21	F3	2010-08-04	7.05	7.82	7.63	6.43	5.33	4.66
22	F3	2010-09-01	6.49	6.43	7.67	6.02	5.16	4.29
23	F3	2010-10-27	4.01	5.39	6.18	1.30	1.26	0.34
24	F3	2010-12-08	2.82	2.28	2.84	1.09	0.61	1.05
25	F3	2011-03-15	0.15	1.44	1.24	0.50	1.13	1.02
26	F3	2011-05-18	1.69	1.03	1.13	1.15	1.13	0.76
27	F3	2011-06-08	3.66	3.11	2.60	2.03	1.57	1.17
28	F3	2011-07-06	6.41	5.58	5.36	5.50	4.03	3.66
29	F3	2011-07-20	7.25	6.98	7.13	6.59	5.41	5.00
30	F3	2011-08-03	9.02	8.00	8.37	8.49	6.25	5.69
31	F3	2011-08-17	6.41	7.03	7.35	5.50	5.48	5.03
32	F3	2011-09-07	9.02	6.52	7.44	8.49	4.94	4.52
33	F3	2011-10-26	5.42	5.53	6.89	2.70	2.18	0.84
34	F3	2011-12-07	4.62	4.56	4.89	0.44	0.22	0.23
35	F3	2012-01-18	2.22	1.88	2.46	0.12	0.12	0.52
36	F3	2012-03-20	2.22	-0.05	0.16	0.12	0.04	0.24
37	F3	2012-04-25	0.27	0.29	0.20	0.25	0.38	0.20
38	F3	2012-05-09	0.67	0.53	0.55	0.20	0.21	0.10
39	F3	2012-08-29	7.67	6.60	7.10	6.66	5.68	4.99
40	F3	2012-12-22	1.73	1.99	2.51	2.02	1.35	1.55

Analysis of Table 3 shows that when considering all profiles, POM with respect to average temperature values m is closer to the observation data than HIROMB in 58% of cases, and with respect to the standard deviation σ - only in 50% of cases. When considering the stations separately, for station BO3 POM is better with respect to m and σ in 58 and 75% of cases, while the estimates for station F3 are 57 and 39%, respectively. In general, from this comparison it can be concluded that the performance in reproducing the water temperature in the Bothnian Bay on coarse grids for both models are about the same.

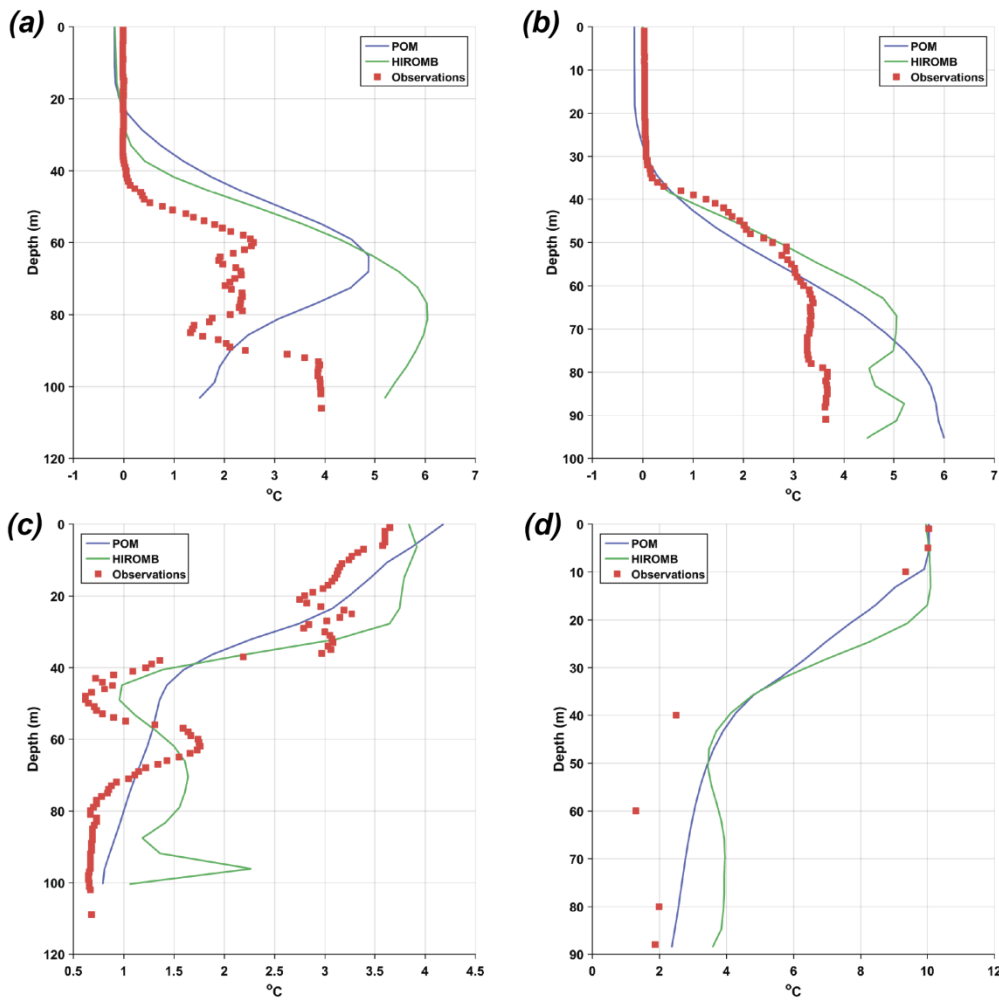


Figure 5: Comparison of the computed temperature profiles by POM and HIROMB with observations provided by BED in the Bothnian Bay. Location of the stations are presented in Fig. 2a. (a) Station BO3, 2010-01-18; (b) Station F3, 2010-01-19; (c) Station BO3, 2010-06-06; (d) Station F3, 2010-06-30.

5

Obviously, the coarse grid with step of 1-2 nm is not able to reproduce the spread of plumes of warm water from the NPP "Hanhikivi-1" discharge point because the characteristic length scale of the plume of the order of 1 km. Proposed in this study the fine nested grid for the vicinity of NPP "Hanhikivi-1" with the steps from 35 to 180 m will allow to solve this problem; i.e. to accurately reproduce the size and shape of thermal pollution plumes around the station. It is important that the solution on the fine grid significantly closer to observational data in comparison with the solution on the coarse grid (see Fig. 6).

10

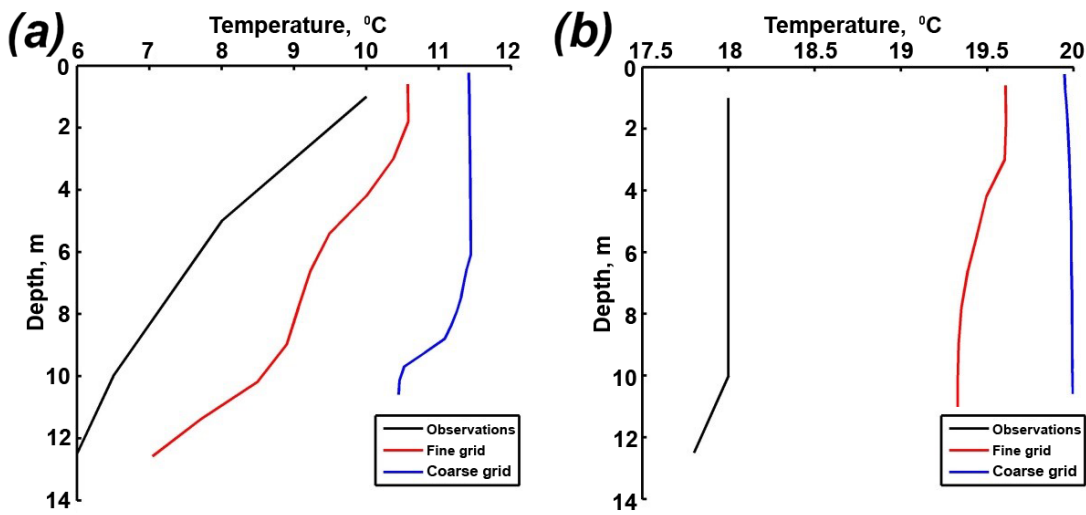
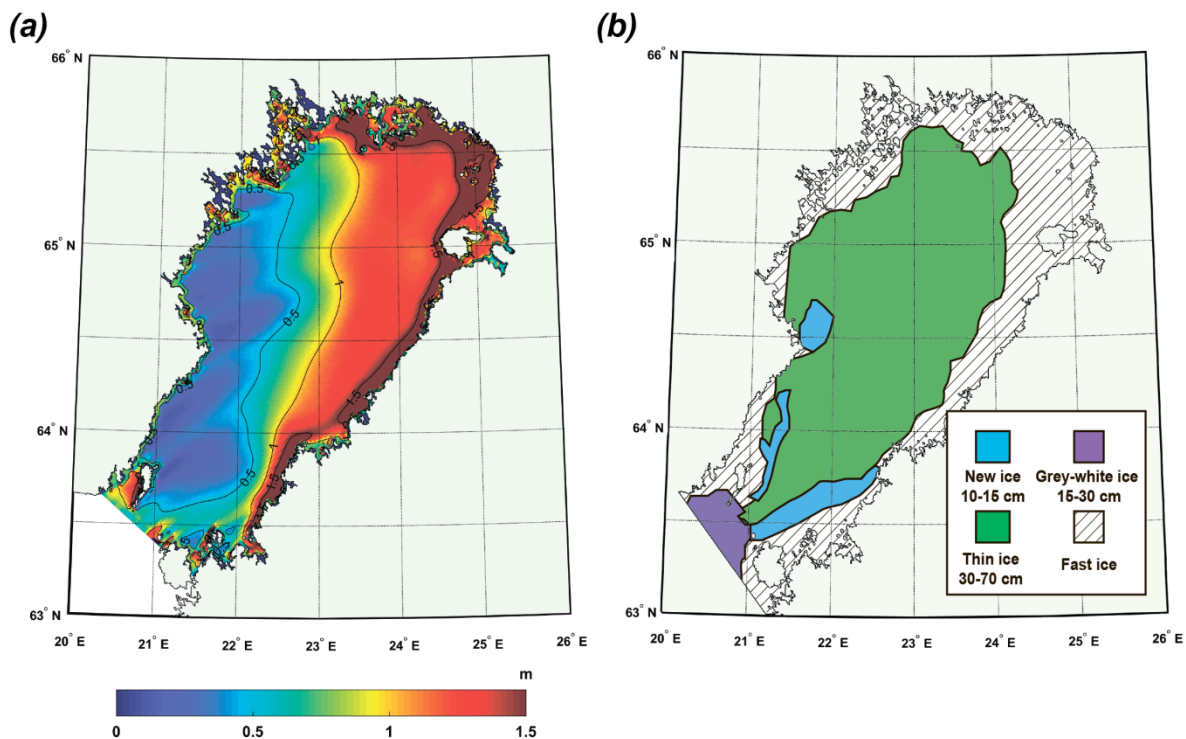


Figure 6: Comparison of the computed temperature profiles by POM on coarse and fine grids (blue and red curves, respectively) with observations (black curves) (Fennovoima report, 2014) at station PP5 near the NPP "Hankikivi-1" in the Bothnian Bay. Location of station PP5 is presented in Fig. 2b. (a) 2010-06-08; (b) 2010-08-03.

5 2.6.2 Sea ice model verification

The comparison of computed sea ice thickness and compactness showed that the model results were in general accordance with observed values (<http://www.aari.ru/>) though some overestimation in ice thickness can be observed (Fig. 7).

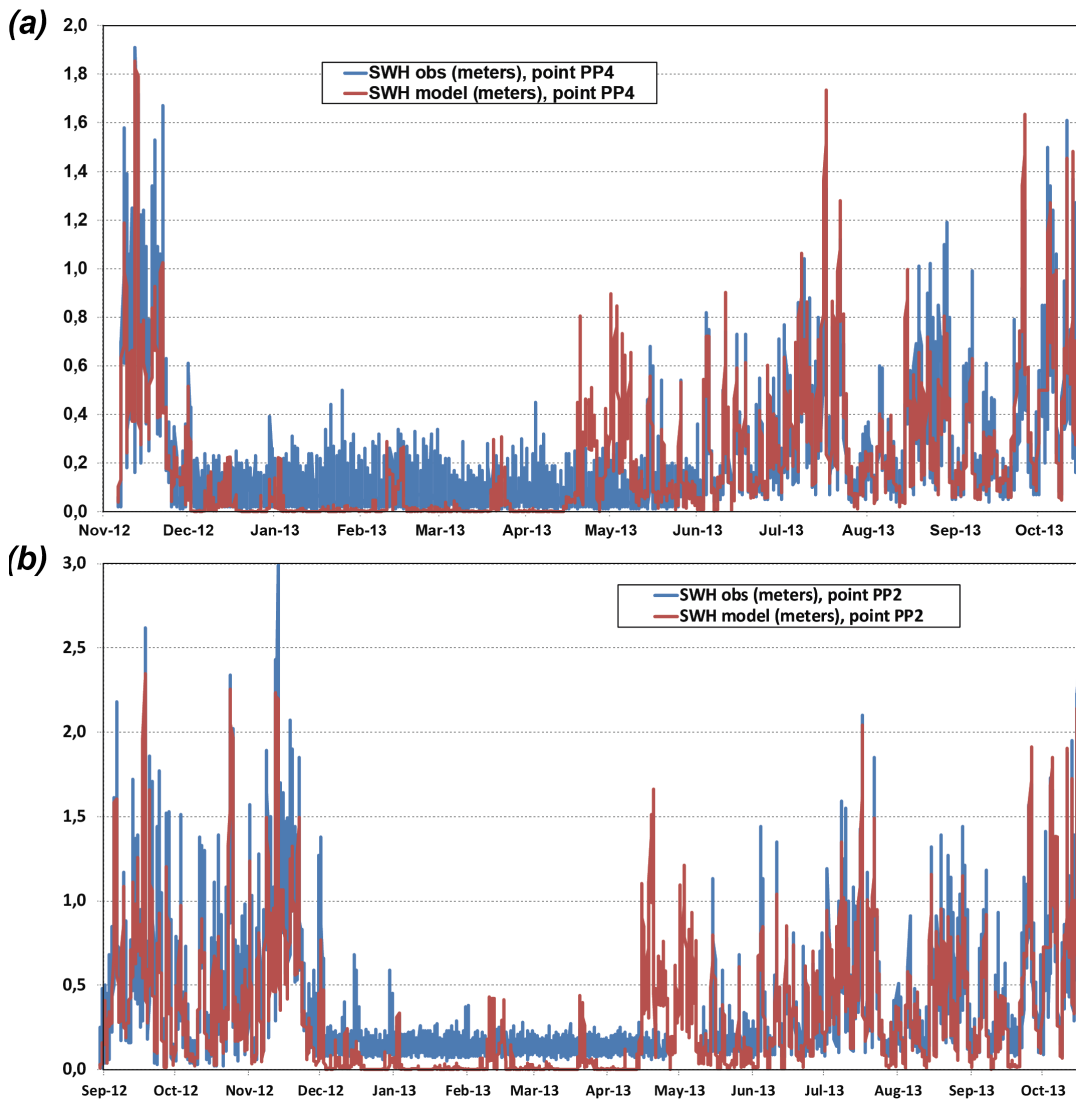


10 Figure 7: Modeled (a) and observed (b) distribution of sea ice thickness in the Bothnian Bay in the period 27 February – 1 March 2011. Ice map in fragment (b) is from the Arctic and Antarctic Research Institute Center "Sever" (St.-Petersburg).

2.6.3 Wind waves model verification

Verification of the results of the SWAN model (in terms of significant wave height – SWH) against observational data (Fennovoima report, 2013) for two points (PP2 and PP4) located in the vicinity of the peninsula Hanhikivi showed that in

general the model correctly simulated wind waves characteristics (Fig. 8). The main discrepancies could be caused by the inaccuracy in dealing with the ice cover in wave model and/or ice cover modeling itself.



5 **Figure 8: Comparison of SWH observations and model results for the period: (a) 06.11.12–17.10.13 and (b) 30.08.12–17.10.13**

Summarizing the above we can say that the proposed POM-based modeling system allows at least not worse than the best model of the Baltic Sea HIROMB to reproduce the principal characteristics of hydrodynamic regime (level, water temperature, altitude wind waves, sea ice) on the coarse grid and gives considerably better description of the temperature field on the fine grid. An advantage of POM important for the prognostic runs is the fact that the POM, unlike HIROMB, is not assimilating observational data.

3 Results

3.1 Modeling of storm events in the vicinity of the future NPP

3.1.1 Wind waves

15 With an aim to assess the maximal possible significant wave heights (SWH) in the area off the Hanhikivi peninsula and to investigate the main features of wind waves field in different hydrometeorological situations a number of numerical experiments with analytically specified different wind speeds and directions was carried out. The area of interest is located along the eastern coast in the Bothnian Bay so we expected that the maximal wind waves would be generated by western

winds. If one drew a hypothetical line along the Bothnian Bay than it would have the direction from south-west to north-east with the angle equal approximately 50 degrees relative to the geographical west-east parallel. Using such line as a coordinate axis we performed 7 main numerical experiments (A-G) with making use of the SWAN model for wind directions varying from 0 to 180 degrees relative to this basic line with angle discretization equal to 30 degrees, wind speed being constant and equal to 10 m s⁻¹ (Fig. 9a).

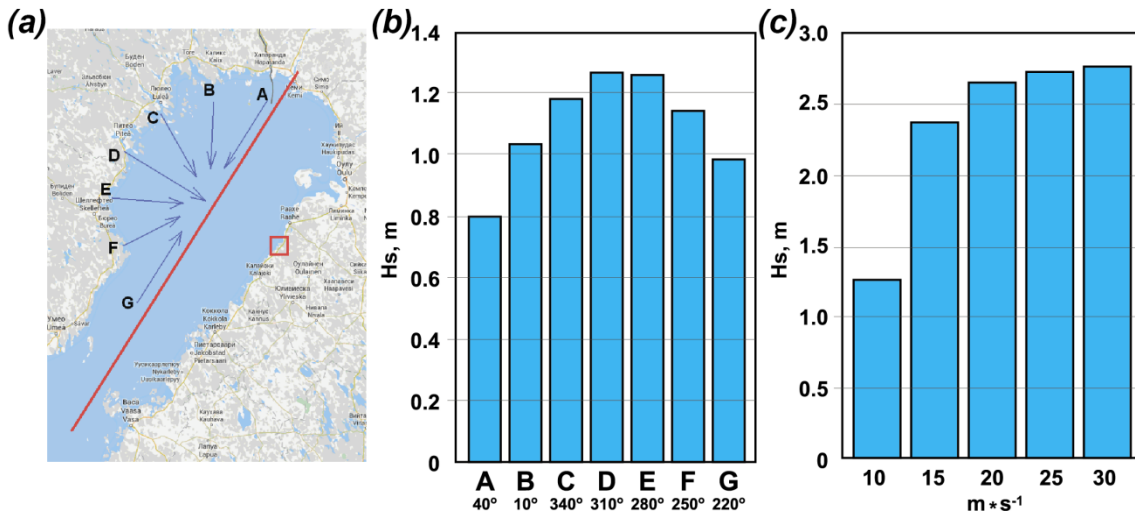


Figure 9: (a) Bothnian Bay imaginary axis (red line), wind direction in numerical experiments (blue arrows) and Hanhikivi peninsula location (red square); (b) Dependence of modeled SWH near NPP upon wind direction; (c) Dependence of modeled SWH near NPP upon wind speed for the most dangerous wind direction (310°).

These wind directions cover the entire range of possible directions capable to produce high waves in the vicinity of the future NPP "Hanhikivi-1". All other wind directions outside the above-mentioned range will lead to the occurrence of wave shadow zone near the Hanhikivi peninsula. Wind duration was 24 h. After the most dangerous wind direction had been determined we used that direction and varied wind speeds holding the direction constant. For that experiment the wind duration was also 24 h.

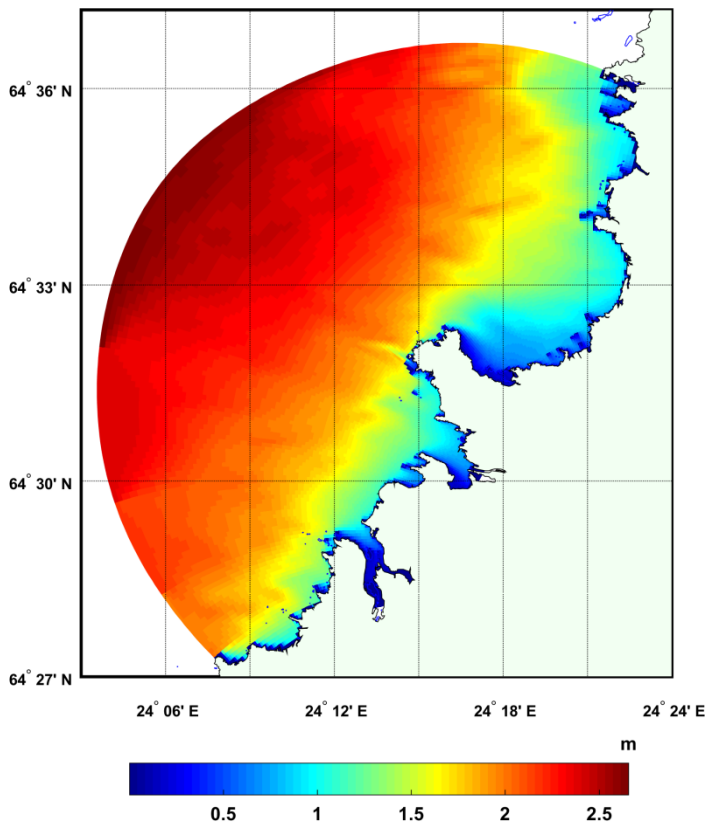
Model calculations of wind waves have shown that the most dangerous in terms of the generation of wind waves in the NPP area is the west and north-west wind with the directions of 280° and 310° (experiments E and D, respectively, Fig. 9b). Maximal SWH in the Bothnian Bay near NPP for that wind direction at a wind speed of 10 m s⁻¹ is about 1.2-1.4 m after 24 hours of wind. Changing the wind speed for the determined most dangerous wind direction (310°) allowed to assess the values of the highest possible wind waves near the NPP (Fig. 9c).

The model results allowed to estimate the values of SWH in both the entire Bothnian Bay and in the small area near Hanhikivi peninsula during different external wind forcing. SWH for the most dangerous wind direction and wind speed of 15 m s⁻¹ was 2.5–3.0 m and increased up to 7.0 m in the open part of the Bothnian Bay for the wind speed of 30 m s⁻¹ (not shown). Nevertheless in the very vicinity of the coast near the Hanhikivi peninsula the SWH decreases dramatically due to relatively shallow depths (see Fig. 2b). It is also interesting to note that considerable increase of SWH in this area in the model experiments appeared during the increase of wind speed from 10 to 15 m s⁻¹ while further wind speed increase did not show such rapid SWH growth (Fig. 9c).

Besides the model experiments with theoretical atmospheric forcing, a model run for the real meteorological forcing of 2014 was carried out for the whole year. Just as in all other numerical experiments, the both models (Bothnian Bay model and Hanhikivi area model) were used: the Bothnian Bay model produced all required wind wave characteristics to be used as boundary conditions in the Hanhikivi area model. The results obtained for 2014 have shown that the highest waves in the Bothnian Bay occurred during the autumn period, SWH reaching 4.0 m. During the winter period of 2014 SWH reached

1.5–2.0 m at ice-free areas of the Bothnian Bay. But the most time during moderate wind speeds SWH was at most 0.5–1.5 m.

A situation with rather large simulated SWH, occurred on the 27 of September 2014, is presented in Fig. 10 in order to show in detail the spatial distribution of waves heights in this area and the influence of bathymetry upon them. The region of the reduction of SWH due to wave breaking and bottom friction is clearly visible and in general coincides with the 5m-isobath. It should be noted that we used the parameterization for bottom friction implemented in the SWAN model, which takes into account the size of bed ripples calculated with making use of available field measurements of grain sizes.



10 **Figure 10: Modeled SWH distribution on the 27 of September, 2014**

Wind waves in the area near the Hanhikivi peninsula can be characterized by the time-series of computed SWH at the location marked by letter "W" in Fig. 2b. The time-series of SWH in the Hanhikivi area for the whole 2014 is presented in Fig. 11.

15

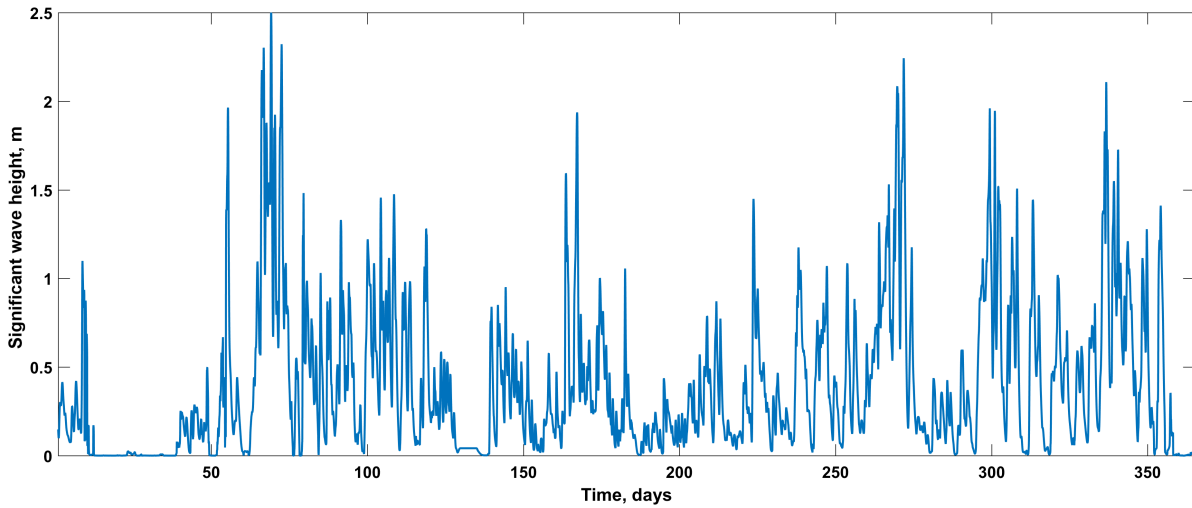


Figure 11: Modeled SWH time-series in the Hanhikivi area at the location mark with "W" on Fig. 2b.

3.1.2 Extreme sea levels

To calculate the extreme sea levels in the vicinity of the NPP "Hanhikivi-1" the maximum possible wind velocity was set equal to 30.2 m s^{-1} (having 0.01 exceedance probability) defined according to the observations in the NPP area (Fennovoima Report, 2015). The wind velocity field calculated using the HIRLAM model was enhanced to reach this maximum wind velocity without any changes in wind direction. The periods of 5–7.12.2015 and 14–16.10.2010 were chosen to simulate the storm surges causing the extreme high and low sea level rise, respectively, because during that periods the real extreme storm surges in the Bothnian Bay were observed. The years 2010–2015 were chosen because we had data for the verification of the model mainly for that period. The results for the entire Bothnian Bay are presented in Fig. 12 for the high level of the storm surge and in Fig 13 for the low level of the storm surge. All computations were performed with making use of the Bothnian Bay coupled circulation model only, without using the nesting technique and the Hanhikivi area model.

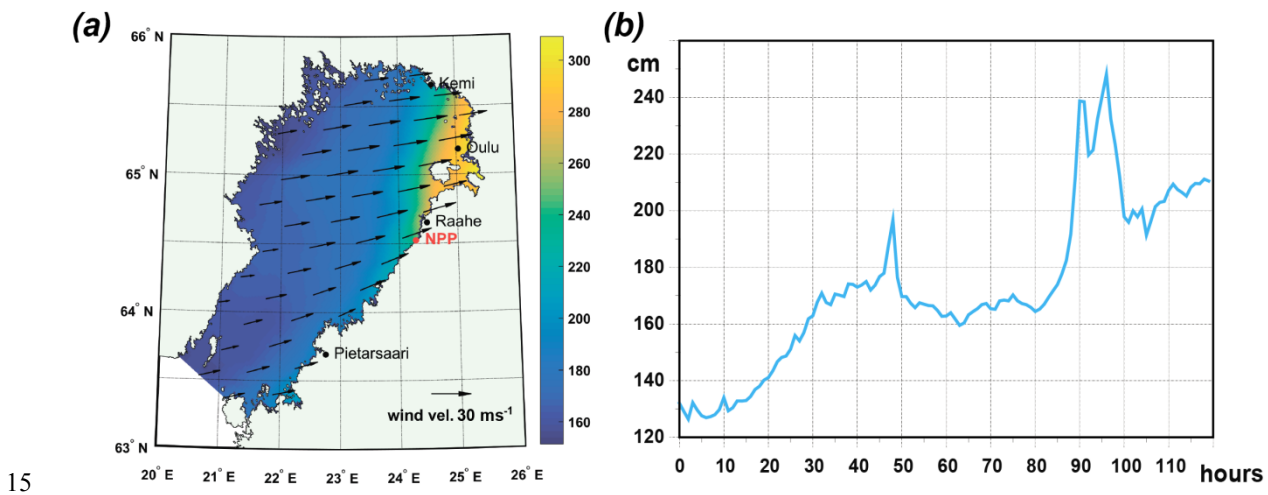


Figure 12: (a) Sea level rise in the Bothnian Bay during the model run with the wind speed 30.2 m s^{-1} and high level of the storm surge; (b) Temporal evolution of sea level rise near the NPP area. X-axis corresponds to the time in hours from the start of the wind.

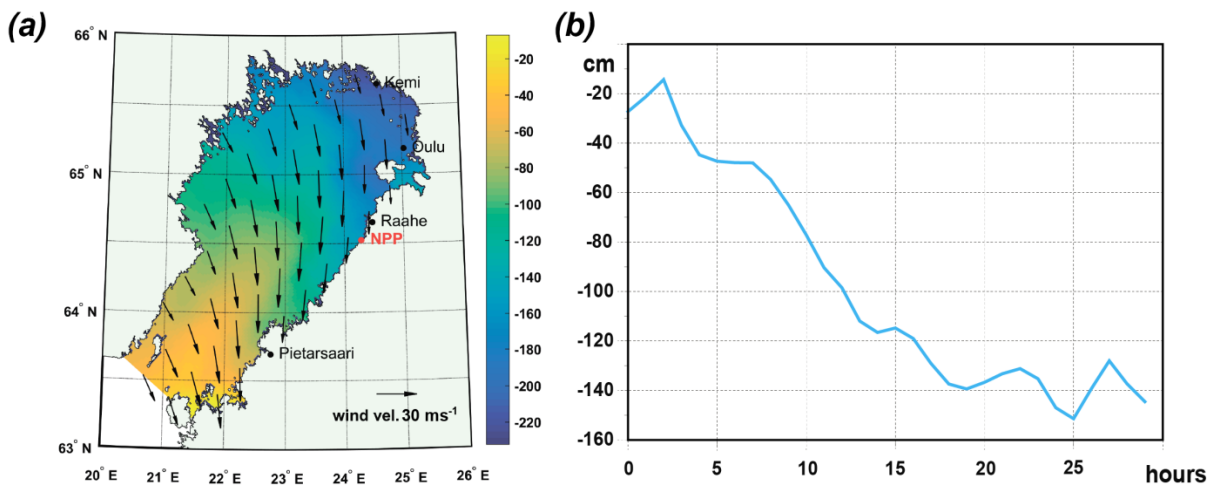


Figure 13: (a) Sea level rise in the Bothnian Bay during the model run with the wind speed 30.2 m s^{-1} and low level of the storm surge; (b) Temporal evolution of sea level rise near the NPP area. X-axis corresponds to the time in hours from the start of the wind.

5

According to the simulations of possible sea level changes in the Bothnian Bay, extreme sea level values in the vicinity of the future NPP at a constant wind of 30.2 m s^{-1} were: maximum of 248 cm and minimum of -151 cm (see Fig. 12b and Fig. 13b). This is in a good agreement with the sea level data for the period 1922-2015 at the station Raahе (Finland) according to the estimates of SMHI (SMHI, 2014) in which the maximal and minimal sea level there could reach up to 250.4 cm and -150 cm, respectively, once in 10^8 years.

10

3.2 Assessment of the thermal pollution of water by the NPP

To assess the possible impacts of the NPP "Hanhikivi -1" on the local thermal regime two scenario runs were performed:

1) "background" scenario: simulating the natural conditions in the absence of the NPP;

15

2) "predictive" scenario: the NPP has been built and is operating with the temperature of heated discharged water set equal to $12 \text{ }^\circ\text{C}$ above the ambient water temperature at the point of water discharge, the discharge being $45 \text{ m}^3 \text{ s}^{-1}$.

Runs were performed for a cold year (2010) and a warm year (2014). The atmospheric characteristics necessary for calculating the fluxes of moment, heat and moisture at the air-water boundary were set according to the atmospheric HIRLAM model with a time resolution of 1 hour. To set the boundary conditions on the open boundary of the Bothnian Bay we used the data from HIROMB model (sea level, water and ice current velocities, temperature, salinity, ice thickness and compactness, snow thickness). The average discharge of river Pohjoishaara was set equal to $33 \text{ m}^3 \text{ s}^{-1}$.

20

In natural conditions, the water of the Gulf around the Peninsula Hanhikivi was covered with ice since the beginning of December to the beginning of May in 2010 (the cold year), and since the beginning of January to the beginning of April in 2014 (the warm year). The highest "background" temperature in the cold and warm year was achieved respectively in July and August. The thermal regime of the basin in the vicinity of the points of water intake and water discharge is almost identical. In general, the spatial variations of mean monthly temperature in the area of the Hanhikivi peninsula limited by radius of 2 km are small, not exceeding $0.6 \text{ }^\circ\text{C}$ for the sea surface temperature (SST) and $1.2 \text{ }^\circ\text{C}$ for the temperature of the deep layer. The main difference between the cold 2010 and the warm 2014 is a longer winter period in 2010.

25

Permanent discharge of warm water in the case of operating NPP will lead to a permanent polynya near the northern tip of the peninsula Hanhikivi resembling in warm winter conditions an ellipse with axes $1.5 \times 6 \text{ km}$, which stretches to the north (Fig. 14b). In cold winter conditions the polynya has a rounded shape, the boundary of which is located from the water discharge point at 2-3 km (Fig. 15b).

30

The difference between "background" and "predictive" model runs is clear. A thermal plume (plume of heated water) emerges in the area of water discharge. Its spatial expansion and propagation mainly depends upon the wind speed and direction above the ice-free water surface and upon the current velocity and direction during ice-cover periods. Figures 14-15 demonstrate the influence of the heated water discharge upon the ice-cover distribution and thickness for both warm 5 (2014) and cold (2010) years, respectively.

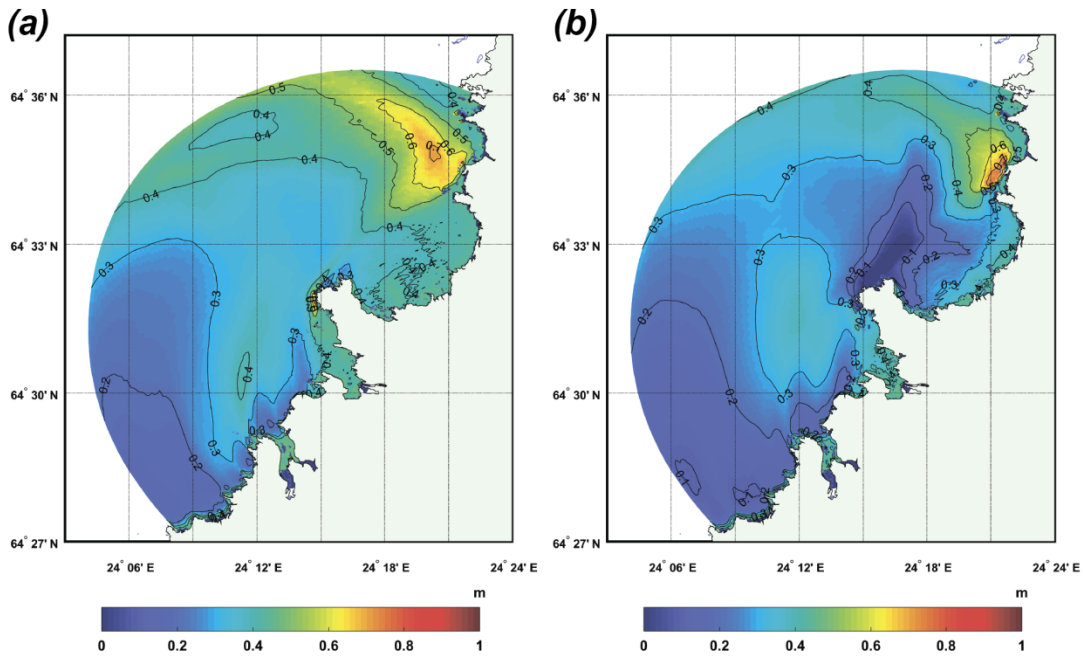


Figure 14: Ice thickness distribution (monthly-mean) in the vicinity of NPP "Hanhikivi-1" in February for conditions of warm year 2014. (a) "background" scenario; (b) "predictive" scenario.

10

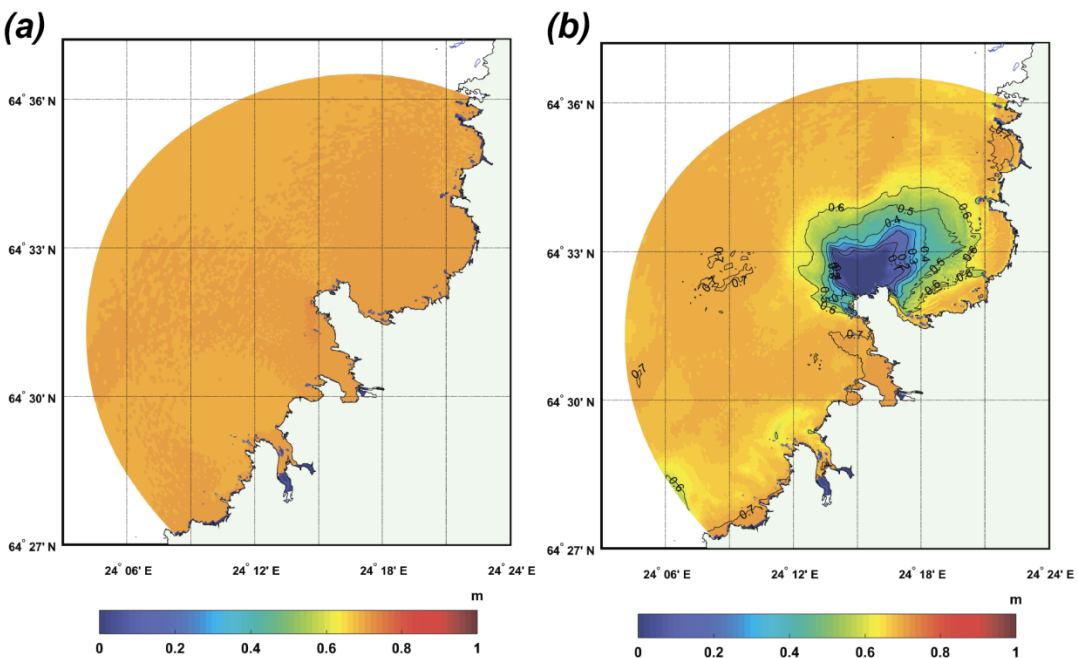


Figure 15: Ice thickness distribution (monthly-mean) in the vicinity of NPP "Hanhikivi-1" in February for conditions of cold year 2010. (a) "background" scenario; (b) "predictive" scenario.

15

A vertical structure of water both in natural conditions and after the construction of the NPP was also investigated. A vertical structure changes significantly when large amounts of heated water have been discharged. Figure 16 shows the

example of vertical cross-sections of the temperature field calculated for the cold year conditions. The position of the cross-section is presented in Fig. 2b, it starts from the heated-water discharge point and stretches to the north. The difference in depth for this one and the same profile is due to the changes in bathymetry caused by the planning hydrotechnical works near the future station.

5

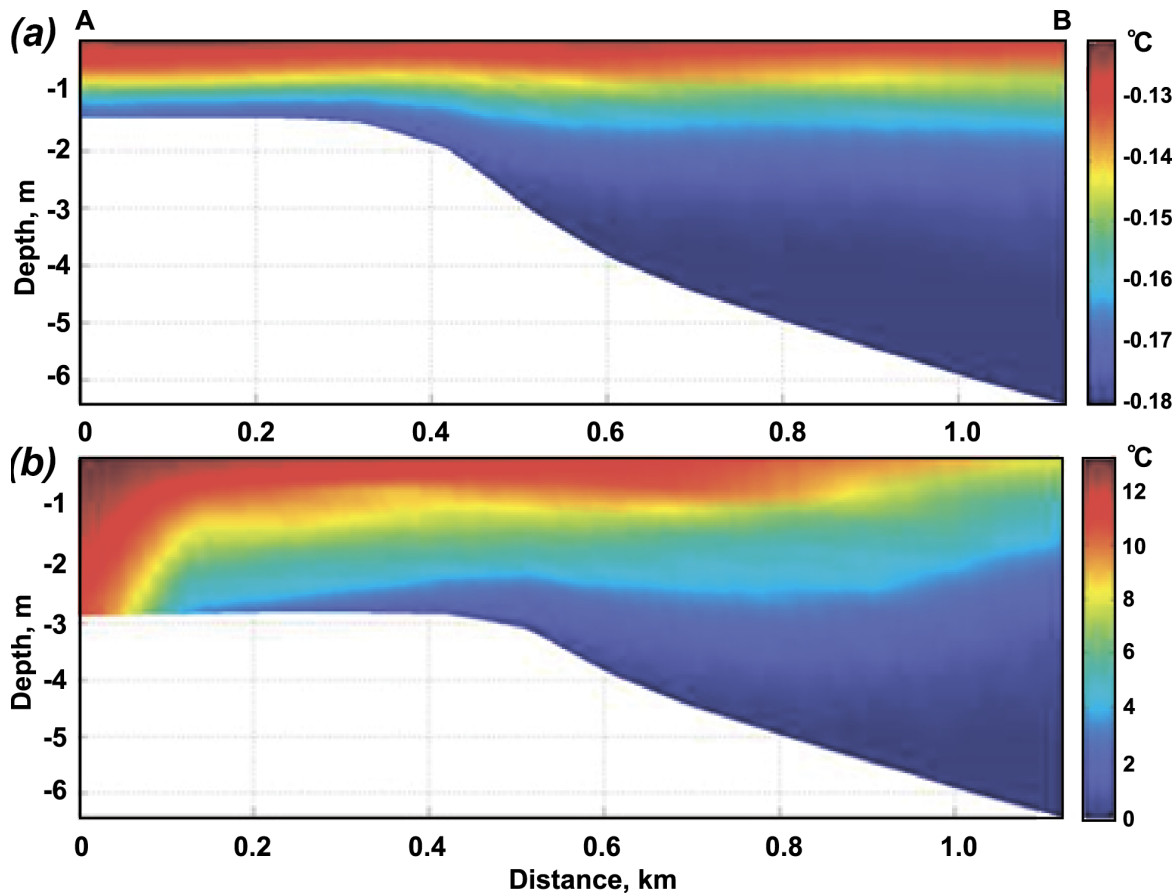


Figure 16: The vertical structure of the temperature field along the section from the discharge point to the north for 04.04.2010: (a) "background" scenario; (b) "predictive" scenario. Temperature scales for (a) and (b) are very different.

10 Thermal regime in the vicinity of the water discharge point becomes completely different: SST deviations from background values are maximal in the 0-250 m zone, where they reach approximately 10 °C in winter and spring and 8 °C in summer and early autumn in cold year (2010). SST deviations decrease with the increasing distance from the water discharge point and reach the minimum value of 0.3 °C in the zone of 1500-2000 m. The bottom water temperature is also maximal in 0-250 m zone, where its deviations amount to 5 °C in winter and spring and 3 °C in summer and early autumn.

15 In the cold year conditions the thermal regime in the case of operating NPP will be changed qualitatively as well as in warm year, but these changes (compared to the background scenario) in the vicinity of both the intake point and the discharge point will be stronger.

4 Discussion

20 Assessment of the scale of the thermal effects which could arise due to the work of NPP "Hanhikivi-1" on the local thermal regime has been obtained for the anomalously warm and cold years. These years for Hanhikivi's area were identified as a result of the statistical analysis of long-term variability of meteorological parameters (with 3-hour resolution) for the period from 1993 to 2014, observed at the meteorological station Raahe Lapaluoto. The data were provided by Fennovoima (Fennovoima report, 2015). It was found that the coldest winter for the period was observed in 2010. The hottest summer for the period 1993 to 2014 was observed in 2002, for the period 2004 to 2014 – in 2014. Choosing 2014 as the abnormally

warm year was dictated by the availability of observational data needed for verification of the models used: the number of available data for 2014 was greater than for 2002. If 2002 would be considered as an abnormally warm year, the difference between the cold and warm years would be more. In any case, the resulting estimates should be viewed only as typical ones that determine the order of magnitude.

5 Another restriction of this study is connected with prescribing the constant temperature difference (12 °C) between the discharged cooling water and the water temperature in the bay. This assumption not taking into account seasonal variations in the temperature of water environment can significantly affect the final result. For example, at the Beloyarsk NPP operating in the Ural Region in the Russian Federation, this difference varies between 9 °C in summer to 12-13 °C in winter (Vereshchagina et al., 2013). Finally, this temperature difference can be set when the plant is operating.

10 The main missing physical mechanism in the coupling of the models used in the present study is the influence of the wave bottom boundary layer upon the current bottom boundary layer. The transfer of SWAN results into the POM model was not made during the computations, only from POM to SWAN. But, from our point of view, this interaction between bottom boundary layers has less impact on the final solution than the influence of meteorological forcing and model estimates of other hydrological parameters such as sea level, sea ice distribution and currents.

15 **5 Concluding remarks**

1. The approach used in this study based on the method of nested grids is well-known in oceanography. Here it has been used together with consideration of: 1) model situations (setting the maximum possible wind of a certain direction in the selected periods of storm surges, prescribing direction and wind speed in the simulation of wind waves) aimed to evaluate the extreme changes in sea level and wind wave parameters in the selected area – the construction area of NPP "Hanhikivi-1" in the Bothnian Bay, Baltic Sea; and 2) the scenarios of "warm" and "cold" years for the detailed assessment of the thermal pollution of the NPP's neighborhood. One important feature of the used nested grids should be emphasized: the grid vertical structure does not change when going from the coarse to the fine grid. This avoids the situation with arising of unstable stratification in fields interpolated on the fine grid and ensures the absence of numerical noise which often causes the instability of computing. The scientific value of this approach is the fact that, unlike traditional statistical estimates of the extreme values of marine characteristics and their repeatability by observations from meteorological stations, it can be used in the local areas where the duration of the time series of observations is small (for example, in high-latitude Arctic seas).

2. The most important results from the engineering point of view for the neighborhood of NPP "Hanhikivi-1" are as follows. Model calculations of wind waves have shown that the most dangerous (in terms of the generation of wind waves in the NPP area) is a north-west wind with the direction of 310°. The maximum height of the waves in the Bothnian Bay near the NPP for this wind direction with wind velocity of 10 m s⁻¹ is 1.2-1.4 m. According to the model estimates, the highest possible level of the sea near the NPP is 248 cm, the minimum level is -151 cm, for the western and eastern winds, respectively. An important feature of thermal pollution around the station is that in the point of water intake for cooling the reactor, in the warm year the sea surface temperature in winter is not lower than the water freezing point and the ice cover is not formed, while in the cold year in the period from the end of December to March in this area there is ice cover with thickness of a few tens of centimeters. Thus, the extreme values of significant wave height, sea level, water temperature in the vicinity of the future NPP "Hanhikivi-1" can be significant and sometimes catastrophic.

3. Numerical experiments for the cold (2010) and the warm year (2014) showed that the permanent release of heat into the marine environment from the operating NPP for the cold year will increase the temperature in the upper layer in 250 m zone (from the heated water discharge point) by 10°C (in average) in winter–spring and by 8°C in summer–early autumn, and in the bottom layer of the same zone by 5°C in winter–spring and 3°C in summer–early autumn. For the warm year, these temperature changes will be smaller. In both cases, in the 1-km vicinity of the station throughout the whole year there is a vertical temperature structure with a pronounced thermocline at a depth of 1-2 meters. Ice cover in both cases will disappear

in two-kilometer vicinity of the NPP. The above warming of the marine environment is important to assess possible changes in the functioning of the natural aquatic ecosystems including fish, when commissioning the NPP, as well as in choosing a site for the creation of aquaculture farms.

4. According to the estimates, the scale of the thermal impact of the NPP on the local thermal regime is substantial and therefore this impact should be taken into account when assessing local climate changes and marine environmental impact in the future.

Competing interests

The authors declare that they have no conflict of interest.

Acknowledgements

10 This study was supported by the Grant N 14-50-00095 of the Russian Science Foundation, by the Grant N 16-55-76021 of the Russian Foundation for Basic Research and by the German Federal Ministry of Education and Research (BMBF) under the research grant 01DJ16016. We would like to thank the Finnish Meteorological Institute for kindly providing us with meteorological and sea level data at station Raahe. We also thank two anonymous reviewers for their helpful comments and suggestions.

15 References

- Abbaspour, M., Javid, A.H., Moghimi, P., Kayhan, K.: Modeling of thermal pollution in coastal area and its economical and environmental assessment, *Int. J. Environ. Sci. Tech.*, Vol. 2, No. 1, 13-26, 2005.
- Acton, J.M., Hibbs, M.: Why Fukushima was preventable, *The Carnegie papers, Nuclear policy*, 44 pp., 2012.
- Alenius, P.: Extremely high sea water temperatures at Hanhikivi-area, Bothnian Bay, in the present climate. FH1-00001248, The Finnish Meteorological Institute, 2015.
- Baltic Sea Hydrographic Commission: Baltic Sea Bathymetry Database version 0.9.3. <http://data.bshc.pro>. Access date: 01.07.2015, 2013.
- Blumberg, A.F. and Mellor, G.L.: A description of a three-dimensional coastal ocean circulation model. In: Heaps, N. (Ed.), *Three-dimensional Coastal Ocean Models*. American Geophysical Union, 208 pp, 1987.
- 25 Booij, N., Ris, R.C., Holthuijsen, L.H.: A third-generation wave model for coastal regions, Part 1. Model description and validation, *Journal of Geophysical Research*, 104 (C4), 7649-7666, 1999.
- Bork, I., Maier-Reimer, E.: On the spreading of power plant cooling water in a tidal river applied to the river Elbe, *Advances in water resources*, Vol. 1, No. 3, 161-168, 1978.
- Buesseler, K., Aoyama, M., Fukasawa, M.: Impacts of the Fukushima Nuclear Power Plants on Marine Radioactivity, *Environmental science and technology*, 45, 9931-9935, 2011.
- 30 Chen, C., Shi, P., Mao, Q.: Application of Remote Sensing Techniques for Monitoring the Thermal Pollution of Cooling-Water Discharge from Nuclear Power Plant, *Journal of Environmental Science and Health, Part A*, 38:8, 1659-1668, 2003.
- Chuang, Y.-L., Yang, H.-H., Lin, H.-J.: Effects of a thermal discharge from a nuclear power plant on phytoplankton and periphyton in subtropical coastal waters, *Journal of Sea Research*, 61, 197-205, 2009.
- Fennovoima report: Vedenlaatu ja virtaukset Hanhikiven edustan vedenottoaikoina O1, O2, O3 ja arkkailupaikoilla PP2, PP4 Tekninen mittausraportti 2011-2013. Fennovoima report. Mikko Kiirikki & Antti Lindfors, Luode Consulting Oy 8.11.2013. 18 pp, 2013.

- Fennovoima report: Environmental Impact Assessment Report for a Nuclear Power Plant. Fennovoima Oy. February, 2014.
- Fennovoima report: Hanhikivi-1 design basis evaluation for external events. Fennovoima report. FH1-00001967. 56 pp, 2015.
- 5 Funkquist, L.: HIROMB, an operational eddy-resolving model for the Baltic Sea, *Bulletin of the Maritime Institute in Gdansk*, Vol. 28, No. 2, 7-16, 2001.
- Haapala, J., Lonroth, N., Stossel, A.: A numerical study of open water formation in sea ice, *Journal of Geophysical Research*, 110, C09011, 2005.
- Hong, Y., Guixiang, D.: Effects of Thermal Discharge from the Coastal Power Plant on the Phytoplankton in
10 Mesocosm Experiments, *Advanced Materials Research*, Vols. 610-613, 3428-3431, 2012.
- Kaplan, E.M., Shvarts, A.A., Luneva, E.V., Makushenko, M.E., Rumynin, V.G.: Transboundary aspect of assessing the impact of NPPs under construction on aquatic ecosystems: Case study of the Baltiiskaya NPP, *Water Resources*, Vol. 43, Issue 7, 911-922, doi:10.1134/S0097807816070046, 2016.
- Lepparanta, M.: A growth model for black ice, snow ice and snow thickness in subarctic basins, *Nordic Hydrology*,
15 14(2), 59-70, 1983.
- Lepparanta, M. and Myrberg, K.: *The Physical Oceanography of the Baltic Sea*. Springer-Verlag, Berlin-Heidelberg-New York, 378 pp, 2009.
- Mellor, G.L.: Users guide for a three-dimensional, primitive equation numerical ocean model. Program in Atmospheric and Oceanic Sciences, Princeton University, Princeton, NJ, 56 pp, 2004.
- 20 Mellor, G.L. and Yamada, T.: Development of a turbulence closure model for geophysical fluid problems, *Reviews of Geophysics and Space Physics*, 20 (4), 851-875, 1982.
- Parkinson, C.L. and Washington, W.M.: A large-scale numerical model of sea ice, *Journal of Geophysical Research*, 84 (C1), 311-337, 1979.
- Ris, R.C., Holthuijsen, L.H., Booij, N.: A third-generation wave model for coastal regions, Part 2. Verification,
25 *Journal of Geophysical Research*, 104 (C4), 7667-7681, 1999.
- Rubbelke, D., Vogeles, S.: (2010), *Impacts of Climate Change on European Critical Infrastructures: The Case of the Power Sector*, BC3 Working Paper Series 2010-08. Basque Centre for Climate Change (BC3). Bilbao, Spain, 23 pp., 2010.
- Rumynin, V.G.: *Overland Flow Dynamics and Solute Transport*, Springer, 287 pp., doi: 10.1007/978-3-319-21801-4, 2015.
- 30 Ryabchenko V.A., Liberman, Yu. M., Ruhovets, L.A., Astrahantsev, G.P., Belevich, M.Yu., Dvornikov, A.Yu., Ignatov, R.Yu., Klevanny, K.A., Mostamandi, S.V., Rubinshteyn, K.G., Tsepelev, V.Yu.: Forecast of the weather and status of water bodies of the North-West Region of Russia on the basis of the complex hydrodynamic models, *Nestor-History*, St. Petersburg, 60 pp, 2008 (in Russian).
- Ryabchenko, V., Dvornikov, A., Haapala, J., Myrberg, K.: Modelling ice conditions in the easternmost Gulf of
35 Finland in the Baltic Sea, *Continental Shelf Research*, 30, 1458-1471, 2010.
- Smagorinsky, J., Manabe, S., Holloway, J.I.: Numerical results from a nine level general circulation model of the atmosphere, *Monthly Weather Review*, 93, 727-768, 1965.
- SMHI, Report No. 2014-18, *Evaluation of Extreme Weather Events in Pyhäjoki, Finland*, SMHI, 36 pp, 2014.
- Srinivasan, T.N., Gopi Rethinaraj, T.S.: Fukushima and thereafter: Reassessment of risks of nuclear power, *Energy*
40 *Policy*, 52, 726-736, 2013.
- Teixeira, T.P., Neves, L.M., Araujo, F.G.: Effects of a nuclear power plant thermal discharge on habitat complexity and fish community structure in Ilha Grande Bay, Brazil, *Marine Environmental Research*, 68, 188-195, 2009.

Tellinghuisen, S.: Energy and Water Nexus. <http://westernresourceadvocates.org/projects/energy-and-water-nexus>.
Access date: 20.11.2016.

Thermal standards for cooling water from new build nuclear power stations. Scientific advisory report series 2011, no 008, British Energy Estuarine and Marine Studies, EDF Energy, 146 pp., 2011.

5 Vereshchagina, E.A., Dvornikov, A.Yu., Rumynin, V.G., Ryabchenko, V.A., Nikulenkov, A.M.: Assessing the impact of Beloyarsk NPP on the hydrothermal regime of the reservoir-cooler, Fundamental and applied hydrophysics, Vol. 6, 4, 58-67, 2013 (in Russian).

von Hippel, F.: The Uncertain Future of Nuclear Energy. Princeton, NJ: Report for International Panel on Fissile Materials, 110 pp, 2010.

10 Zeng, P., Chen, H., Ao, B., Ji, P., Wang, X., Ou, Z.: Transport of waste heat from a nuclear power plant into coastal water, Coastal Engineering, 44, 301-319, 2002.

Table 1: Statistical characteristics of air temperature, atmospheric pressure and wind speed in the surface layer of the atmosphere between 2010 and 2014, calculated on the average daily data

Years	Air temperature, °C		Atmospheric pressure, mb		Wind velocity, m c ⁻¹	
	Observations	HIRLAM	Observations	HIRLAM	Observations	HIRLAM
	Mean annual value					
2010	2.1	2.0	1012.2	1012.6	5.5	4.7
2011	4.6	3.7	1009.0	1009.5	6.3	5.5
2012	3.1	3.2	1010.3	1010.7	5.8	6.1
2013	4.7	4.7	1010.2	1010.6	6.2	6.1
2014	5.2	5.1	1012.8	1013.0	6.1	6.1
	Minimum value					
2010	-27.4	-26.5	981.8	981.6	1.5	1.1
2011	-25.6	-26.9	969.3	970.4	1.2	0.9
2012	-24.7	-26.1	973.2	973.4	1.7	1.9
2013	-19.2	-20.1	974.9	976.1	2.0	1.0
2014	-20.0	-21.9	976.5	977.3	1.7	1.6
	Maximum value					
2010	26.0	24.7	1046.8	1046.3	11.6	13.1
2011	25.6	20.4	1037.4	1038.0	18.9	17.2
2012	20.1	20.1	1056.0	1055.7	13.2	14.6
2013	21.4	21.3	1033.6	1033.9	17.7	18.1
2014	25.8	24.7	1040.6	1040.1	14.7	15.6
	Standard deviation					
2010	11.4	12.0	11.3	11.2	2.2	2.1
2011	9.9	9.0	12.8	12.7	2.8	2.9
2012	9.7	9.9	13.0	12.9	2.3	2.5
2013	9.4	9.2	10.7	10.7	2.5	2.8
2014	8.8	9.1	11.8	11.6	2.7	2.8

Table 2: Statistical characteristics (correlation coefficient R and standard deviation σ) of water level at coastal stations in the Bothnian Bay in 2010-2015 according to observations, results from HIROMB and POM (this study)

Characteristic	R , data – POM	R , data– HIROMB	σ , m data	σ , m POM	σ , m HIROMB
Ratan	0.88	0.88	0.24	0.21	0.22
Furuogrund	0.88	0.89	0.25	0.22	0.24
Kalix	0.88	0.88	0.27	0.24	0.25
Kemi	0.89	0.90	0.28	0.25	0.27
Raahe	0.88	0.89	0.23	0.26	0.25
Pietarsaari	0.80	0.82	0.21	0.22	0.23

Table 3: Statistical characteristics (mean value m and standard deviation σ) of vertical temperature profiles at the oceanographic stations BO3 and F3 in the Bothnian Bay in 2010-2012 according to BED observations, results from HIROMB and POM (this study)

Station Number	Station Name	Station Date	$m, ^\circ C$ Data	$m, ^\circ C$ HIROMB	$m, ^\circ C$ POM	$\sigma, ^\circ C$ Data	$\sigma, ^\circ C$ HIROMB	$\sigma, ^\circ C$ POM
1	BO3	2010-01-18	1.29	2.90	2.02	1.36	2.64	1.77
2	BO3	2010-01-18	0.60	1.44	0.53	0.56	1.43	0.57
3	BO3	2010-06-06	1.73	2.20	1.89	1.10	1.14	1.11
4	BO3	2010-08-22	4.05	6.50	7.11	4.80	5.16	4.56
5	BO3	2011-01-24	0.82	1.47	0.76	0.88	1.10	0.67
6	BO3	2011-05-29	1.30	1.92	1.76	1.01	1.56	1.23
7	BO3	2011-08-21	5.76	6.37	8.34	4.65	6.01	4.64
8	BO3	2012-05-31	1.99	2.71	2.93	1.07	1.49	1.17
9	BO3	2012-08-23	6.13	7.83	8.38	4.13	4.85	3.98
10	BO3	2010-12-02	3.61	2.91	3.01	0.44	1.14	1.32
11	BO3	2011-12-11	3.30	2.92	3.53	0.52	0.80	0.17
12	BO3	2012-12-10	3.58	3.93	4.08	0.39	1.21	1.21
13	F3	2010-01-19	1.74	2.45	2.41	1.53	2.22	2.47
14	F3	2011-01-24	0.95	1.14	1.27	0.93	1.08	1.29
15	F3	2010-03-05	0.41	2.14	1.81	1.12	2.28	1.79
16	F3	2010-03-23	0.73	1.91	1.92	1.09	2.04	1.95
17	F3	2010-05-05	0.92	2.44	2.29	1.11	1.94	1.67
18	F3	2010-05-19	1.29	2.22	2.20	0.88	1.78	1.44
19	F3	2010-06-09	3.74	3.53	2.94	2.79	0.34	0.72
20	F3	2010-06-30	5.30	5.76	5.07	4.24	2.71	2.75
21	F3	2010-08-04	7.05	7.82	7.63	6.43	5.33	4.66
22	F3	2010-09-01	6.49	6.43	7.67	6.02	5.16	4.29
23	F3	2010-10-27	4.01	5.39	6.18	1.30	1.26	0.34
24	F3	2010-12-08	2.82	2.28	2.84	1.09	0.61	1.05
25	F3	2011-03-15	0.15	1.44	1.24	0.50	1.13	1.02
26	F3	2011-05-18	1.69	1.03	1.13	1.15	1.13	0.76
27	F3	2011-06-08	3.66	3.11	2.60	2.03	1.57	1.17
28	F3	2011-07-06	6.41	5.58	5.36	5.50	4.03	3.66
29	F3	2011-07-20	7.25	6.98	7.13	6.59	5.41	5.00
30	F3	2011-08-03	9.02	8.00	8.37	8.49	6.25	5.69
31	F3	2011-08-17	6.41	7.03	7.35	5.50	5.48	5.03
32	F3	2011-09-07	9.02	6.52	7.44	8.49	4.94	4.52
33	F3	2011-10-26	5.42	5.53	6.89	2.70	2.18	0.84
34	F3	2011-12-07	4.62	4.56	4.89	0.44	0.22	0.23
35	F3	2012-01-18	2.22	1.88	2.46	0.12	0.12	0.52
36	F3	2012-03-20	2.22	-0.05	0.16	0.12	0.04	0.24
37	F3	2012-04-25	0.27	0.29	0.20	0.25	0.38	0.20

38	F3	2012-05-09	0.67	0.53	0.55	0.20	0.21	0.10
39	F3	2012-08-29	7.67	6.60	7.10	6.66	5.68	4.99
40	F3	2012-12-22	1.73	1.99	2.51	2.02	1.35	1.55

Figure Captions

Figure 1: The general scheme of the model calculations.

Figure 2: Bathymetry of the Bothnian Bay (a) and the area off the Hanhikivi peninsula (b). The location of the NPP, oceanographic stations (BO3, F3, PP2, PP4, PP5), coastal sites of sea-level measurements (Ratan, Furuogrund, Kalix, Kemi, Raahe, Pietarsaari) and also the position of cross-section (red line) and SWAN output point (W) are presented. The inset in the fragment (a) shows the position of the Bothnian Bay in the Baltic Sea.

Figure 3: Temporal variability of mean monthly values of (a) air temperature ($^{\circ}\text{C}$), (b) atmospheric pressure (mb) and (c) wind speed (m s^{-1}) in the near-surface layer of the atmosphere. HIRLAM (dashed curves), observations (green curves).

Figure 4: Comparison of POM and HIROMB calculated sea levels at station Raahe located near the NPP "Hankikivi-1" for the storm surge periods of 14-16.10.2010 (a) and 5-7.12.2015 (b).

Figure 5: Comparison of the computed temperature profiles by POM and HIROMB with observations provided by BED in the Bothnian Bay. Location of the stations are presented in Fig. 2a. (a) Station BO3, 2010-01-18; (b) Station F3, 2010-01-19; (c) Station BO3, 2010-06-06; (d) Station F3, 2010-06-30.

Figure 6: Comparison of the computed temperature profiles by POM on coarse and fine grids (blue and red curves, respectively) with observations (black curves) (Fennovoima report, 2014) at station PP5 near the NPP "Hankikivi-1" in the Bothnian Bay. Location of station PP5 is presented in Fig. 2b. (a) 2010-06-08; (b) 2010-08-03.

Figure 7: Modeled (a) and observed (b) distribution of sea ice thickness in the Bothnian Bay in the period 27 February – 1 March 2011. Ice map in fragment (b) is from the Arctic and Antarctic Research Institute Center "Sever" (St.-Petersburg).

Figure 8: Comparison of SWH observations and model results for the period: (a) 06.11.12–17.10.13 and (b) 30.08.12–17.10.13

Figure 9: (a) Bothnian Bay imaginary axis (red line), wind direction in numerical experiments (blue arrows) and Hanhikivi peninsula location (red square); (b) Dependence of modeled SWH near NPP upon wind direction; (c) Dependence of modeled SWH near NPP upon wind speed for the most dangerous wind direction (310°).

Figure 10: Modeled SWH distribution on the 27 of September, 2014

Figure 11: Modeled SWH time-series in the Hanhikivi area at the location mark with "W" on Fig. 2b.

Figure 12: (a) Sea level rise in the Bothnian Bay during the model run with the wind speed 30.2 m s^{-1} and high level of the storm surge; (b) Temporal evolution of sea level rise near the NPP area. X-axis corresponds to the time in hours from the start of the wind.

Figure 13: (a) Sea level rise in the Bothnian Bay during the model run with the wind speed 30.2 m s^{-1} and low level of the storm surge; (b) Temporal evolution of sea level rise near the NPP area. X-axis corresponds to the time in hours from the start of the wind.

Figure 14: Ice thickness distribution (monthly-mean) in the vicinity of NPP "Hanhikivi-1" in February for conditions of warm year 2014. (a) "background" scenario; (b) "predictive" scenario.

Figure 15: Ice thickness distribution (monthly-mean) in the vicinity of NPP "Hanhikivi-1" in February for conditions of cold year 2010. (a) "background" scenario; (b) "predictive" scenario.

Figure 16: The vertical structure of the temperature field along the section from the discharge point to the north for 04.04.2010: (a) "background" scenario; (b) "predictive" scenario. Temperature scales for (a) and (b) are very different.